

THREE-DIMENSIONAL EVOLUTION OF  
MERCURY'S SPIN-ORBIT RESONANCE

by

Norman Brenner

B.A., Central High, Phila., 1961

A.B., Princeton, 1964

M.A., Harvard, 1972

SUBMITTED IN PARTIAL FULFILLMENT

OF THE REQUIREMENTS FOR THE

DEGREE OF DOCTOR OF PHILOSOPHY

at the

MASSACHUSETTS INSTITUTE OF TECHNOLOGY

June, 1975

Signature of Author

Signature redacted

Department of Earth and Planetary Sciences  
28 February 1975

Certified by

Signature redacted

Thesis Supervisor

Certified by

Signature redacted

Thesis Supervisor

Accepted by

Signature redacted

Chairman, Departmental Graduate Committee



## ACKNOWLEDGEMENTS

I would like to thank my two advisors, Professors Shapiro and Counselman, for their assistance in choosing and in carrying out this thesis research. I would also like to thank my wife, but this is impossible, as I am single.

This work was supported in part by a National Science Foundation fellowship.

# THREE-DIMENSIONAL EVOLUTION OF MERCURY'S SPIN-ORBIT RESONANCE

by

Norman Brenner

Submitted to the Department of Earth and Planetary Sciences in June, 1975 in partial fulfillment of the requirement for the degree of Doctor of Philosophy.

## ABSTRACT

Previous investigations of the evolution of the 3:2 spin-orbit resonance state of the planet Mercury have used simplified mathematical models in which the rotation axis of the planet has been assumed to remain perpendicular to the orbital plane. This thesis investigates the evolution of both the spin rate and the orientation of the rotation axis under tidal and permanent-asymmetry torques applied by the Sun. It is found that as the spin rate decreases, the inclination of the equatorial to the orbital plane increases. For initial inclinations of less than  $50^\circ$ , the maximum inclination is never greater than  $60^\circ$ , and is attained when the spin rate is about three times the orbital mean motion. The effect of such a substantial inclination upon the resonance capture probability depends upon the tidal-friction model. For a viscous friction model, the capture probability is less at each resonance for non-zero inclination than for the previously studied, zero inclination, case. However, for a model in which the tidal torque undergoes a discrete change with passage through the resonant rotation rate, the capture probability is less for non-zero inclination for the odd-half-integer resonances (3:2, 5:2, etc.), and larger for the even resonances (2:1, 3:1, etc.). Also, the capture probabilities for the discrete-change model are consistently larger (approximately one) than probabilities for the viscous model. If for this reason, the step model should be preferred to the viscous model, the question is raised: why was not Mercury trapped in the 2:1 or 3:1 resonance state?

Thesis supervisors:

Irwin I. Shapiro, Ph.D.

Title: Professor of Geophysics and Physics

Charles C. Counselman, Ph.D.

Title: Professor of Planetary Science

## CURRICULUM VITAE

Norman Brenner was born in Philadelphia, Pennsylvania on 2 December 1944. He graduated from Central High School, Philadelphia, with a B.A. in 1961, and from Princeton University, Princeton, New Jersey, with an A.B. in Mathematics in 1964. He attended Harvard University from 1964 to 1965 and received an M.A. in Applied Mathematics in 1972. He has been enrolled in the Department of Earth and Planetary Sciences at Massachusetts Institute of Technology since 1968.

His graduate study has been supported by a National Science Foundation Traineeship (1964-65) and Scholarship (1969-73), by an M.I.T. Research Assistantship (1969) and Teaching Assistantship (1972-74). He worked at the M.I.T. Lincoln Laboratory, Haystack Microwave Research Facility from 1965 to 1968, and at the International Business Machines Thomas J. Watson Sr. Research Laboratory in the summers of 1969, 1970 and 1971.

He won the 1st M.I.T. Spelling Bee in 1975.

## TABLE OF CONTENTS

Acknowledgements	2
Abstract	3
Curriculum Vitae	4
Table of Contents	5
I. Introduction to the Problem	7
Review of the physics	9
Mathematical precis	12
II. The Mathematical Model	17
The two torques	17
The long slowdown	20
The coordinate systems	22
The torque equation	22
The angular momentum	22
The torque	24
The inertia coefficients	27
III. Time Averaging and Elasticity Models	29
Magnitude of terms	29
Time averaging	30
Averaged asymmetry torque	32
Averaged tidal torque	33
Qualitative changes in time	34
Models for phase lag	35
IV. Resonance Capture	38
Capture probabilities	40

V. Discussion of Results	44
Qualitative estimates	44
Evolution by numerical integration	47
Resonance capture probabilities	50
Bibliography	53
Appendices	
A. The Wigner Rotation Coefficients	56
B. Spherical Harmonics and Inclination Polynomials	64
C. Hansen Coefficients	67
D. Generalized Inertia Coefficients	70
E. Comparison with Peale's Paper	74
Figure Captions	77
Figures	79

## CHAPTER I. Introduction to the problem

Until 1965, Mercury was thought to rotate once sidereally per one 88 day orbit (Allen, 1964). Therefore, it would always present nearly the same face to the sun. Pettengill and Dyce (1965) showed from delay-Doppler radar data that the rotation period was actually  $59 \pm 5$  days. Subsequently, Colombo (1965) proposed that the rotation period was "locked" at exactly  $2/3$  of the orbital period, or about 59 days. Colombo and Shapiro (1965), Goldreich and Peale (1966) and Counselman (1969) among others have analyzed the process of capture into this locked-in rotation mode. For simplicity's sake, in all of these analyses it was assumed that Mercury's spin axis has always been perpendicular to its orbit plane. I now relax this assumption and examine the consequences. Just prior to the presentation of this thesis, Peale (1974) published many of the same results, which he obtained independently. The main points of agreement or disagreement between his and my results will be presented in Appendix E.

The mathematics in what follows is complicated for three reasons. First, three-dimensional vector equations necessarily replace the one degree of freedom equations of the theoretical papers mentioned above. Further, three separate sets of (moving) coordinate axes are important: 7 a set fixed in the planet, a set

fixed with respect to the planet's equatorial plane, and one which is fixed with respect to the orbit plane. Second, the functions for the torques are expanded into spherical harmonic series in spatial variables and Fourier series in time. Third, two different types of models for the tidal torque are considered. As a guide through the algebraic formalism, a precis of the mathematics is given first; then a more complete development, with the detailed calculations being shown in the appendices. I will also present physical interpretations of the mathematical results whenever I can.



## Review of the physics

Mercury travels in a moderately elliptical orbit very near the Sun. Both factors contribute to the strength of the spin-orbit resonance. Currently, the orbit eccentricity is about .20 but it is thought to vary between .12 and .24 over millions of years due to planetary perturbations (Brouwer & van Woerkom, 1950). Similarly, the orbit plane is regressing around an inertial axis once in 400,000 years, with a variable inclination to that axis of never more than  $10^\circ$ . Perihelion is advancing in the orbit plane about one cycle in 200,000 years, while the semi-major axis is essentially constant at  $60 \times 10^9$  m. The mean motion (orbital angular speed)  $n$  equals  $2\pi/(88 \text{ day})$ ; the spin rate now is about  $1.5n$ . The spin axis currently is inclined less than  $10^\circ$  from the orbit plane. The spin axis precession period around the orbit normal is perhaps  $10^5$  years, a value I will estimate below.

We do not know the original spin period of Mercury. The planets Mars through Neptune have undergone little tidal braking, and their periods currently range from 10 to 24 hours. Mercury's may once have been about 20 hours. Similarly, we do not know the original inclination of the spin axis, and the other planets exhibit a wide range of inclinations.

The Sun raises tides in the solid body of Mercury. These tides follow the sun around the planet, dissipating energy through inelasticity. Therefore, the Sun exerts a torque on Mercury through these tidal "bulges". If Mercury has not always been in a resonance, then it must have been slowed

down by this tidal torque, over a time of the order of  $10^7$  to  $10^9$  years. If unchecked by a countertorque, the slowdown would not stop until a spin rate were attained for which the average tidal torque exerted by the Sun on the planet in one orbit is zero. For different tidal models, estimates of this equilibrium rate range from  $n$  to nearly  $1.5n$ . Yet Mercury revolves faster than this, apparently at exactly  $1.5n$ , or three turns in two orbits. What stabilized this higher rate?

The widely accepted answer is that Mercury, even without tidal strain, is not axially symmetric, but has a difference between its two equatorial principal moments of inertia. When the spin rate is  $1.5n$ , the longer equatorial axis of Mercury points at the Sun exactly three times per orbit. The Sun's torque on the permanent asymmetry (called the "asymmetry torque" for short) may not average to zero over an orbit, depending on the orientation of the long axis at perihelion passage. Indeed, such an effect occurs when the spin rate is any nonzero integral or half-integral multiple of  $n$ . However, only the low-numbered resonances are strong enough possibly to stabilize the spin against the deceleration of the tidal torque.

The following is a crude analogy to capture; the very important matter of spin phase angle is not brought out clearly. However, I have found this analogy helpful. Picture a ball rolling down a mountain to a valley below. Its height corresponds to the spin rate of Mercury. The slope of the mountain represents the tidal torque, and the valley represents the

equilibrium spin rate where the average tidal torque vanishes. Periodically spaced ledges on the side of the mountain slow the ball's descent, but all save the bottommost few ledges slope downwards, so that except for the latter, no ledge can trap the ball. The ledges represent the asymmetry torque, which averages to zero, except at select values of the spin rate. Near the bottom, a few ledges are broader and upward-sloping; if the ball could somehow lose its accumulated kinetic energy, it could fall back and be captured in the crook of a ledge. Therefore capture at a resonance rate above equilibrium requires both a strong asymmetry torque (upward sloping ledge) and a dissipation mechanism of a certain kind.

It will be shown that the likelihood of capture depends upon the spin phase angle of Mercury, that is, the angle of the rotating equatorial axes relative to an inertial frame. The value of this phase angle at the times of possible captures is completely unknown, of course. Since only certain ranges of the phase angle will lead to capture, we can only compute probabilities of capture.

In summary, the tidal torque decelerates the planet. As the spin rate passes near a whole- or half-integral multiple of the mean motion  $n$ , the strong asymmetry torque averages to a non-zero value and attempts to brake the deceleration. The effect of a non-zero inclination of the equatorial plane to the orbit plane will be investigated here to determine how it may affect capture probabilities.

### Mathematical precis

A summary of the mathematical arguments will now be given.

The fundamental equation governing the rotation of Mercury is that the change in the angular momentum of the planet is equal to the applied torque:

$$\frac{d\mathbf{H}}{dt} = \mathbf{T}$$

The angular momentum  $\mathbf{H}$ , as seen from an inertial coordinate system, is the sum of the rotational and the orbital angular momenta. However, the applied torque in this situation is far too weak to affect the orbital angular momentum significantly. To our degree of approximation, we shall consider the spin angular momentum to be solely in the direction of Mercury's principal axis of inertia. The time derivative of  $\mathbf{H}$  breaks up, therefore, into two major components. One is due to the deceleration of the spin; this component of  $\mathbf{H}$  is in the direction of the spin axis. The other is due to the precession and nutation of the spin axis; this component is perpendicular to the spin axis.

The torque  $\mathbf{T}$  of the Sun on Mercury is

$$\mathbf{T} = -M_{\odot} \mathbf{R} \times \mathbf{F}$$

where  $M_{\odot}$  is the Sun's mass,  $\mathbf{R}$  is the vector from Mercury to the Sun, and  $\mathbf{F}$  is the force per unit mass that Mercury exerts on the Sun. If the origin of coordinates is at Mercury's center of mass, and if Mercury is perfectly spherical, it can exert no net torque on the Sun. Therefore we must calculate the devi-

ations from sphericity of Mercury.

Mercury possesses permanent asphericities such as a polar flattening, mountain ranges, etc., and temporary, tidally-caused ones. The order of magnitude of the permanent ones may be estimated by comparison with the Moon; the tidal deviations may be estimated by computing the tidal distortions of an elastic body. The nature of the elasticity model makes a great difference in the final results; two representative models are used, one which leads to a tidal torque varying continuously with spin rate, and one which leads to step-like variations.

In any event, the torque can be expressed as a sum of spherical harmonic functions  $Y_{\ell m}(\Theta, \Phi)$  where the angles  $\Theta$  and  $\Phi$  are the spherical coordinates of the Sun as seen from a Mercurian coordinate system. The coefficients of the spherical harmonics depend upon the asphericities.

Our single vector differential equation (Euler's equation) can thus be split along the coordinate axes into three scalar, simultaneous differential equations, of which a typical one is

$$\frac{d^2\psi}{dt^2} = \sum_{\ell m} A_{\ell m} Y_{\ell m}(\Theta, \Phi)$$

where  $\psi$  is the phase angle of the planet's spin. This is the equation representing the deceleration of Mercury under the applied torque. Before we try to solve it and the other two equations, we must note two points.

First, that the coefficients  $A_{\ell m}$  depend upon the spin angles of Mercury ( $\psi$  and the angles defining the position of the spin axis in space). Secondly, these angles (except  $\psi$ ) are changing only very slowly. We are not interested here in

their short term changes, i.e. the changes over time scales comparable to the period of Mercury's orbit, but in their secular changes, over thousands of orbit periods. This secular change may be isolated by averaging both sides of our equations over many orbit periods. To facilitate this time averaging, we first must further expand the right hand sides, principally the  $Y_{\ell m}$  terms, into Fourier series with time as the independent variable.

The expansion into Fourier series of the torque expressions makes manifest the dependence on the spin angles. Besides the angle  $\psi$  of spin phase, there are also the angles  $\theta$  and  $\varphi$  which are the spherical coordinates of the direction of the spin axis with respect to an orbital coordinate system. After expansion, but before averaging, the torque expressions on the right hand side of our differential equations look like the following typical sum:

$$\sum_{\ell m} B_{\ell m}(\theta, \varphi, e, \Omega, \iota, \omega) \exp(i\ell t + im\psi)$$

The coefficient  $B_{\ell m}$  depends on  $\theta$  and  $\varphi$ , on  $e$ , the orbit eccentricity and on  $(\Omega, \iota, \omega)$ , the Euler angles defining the orientation of the orbit with respect to inertial coordinates. The dependence on  $\theta$ , the inclination angle of the spin axis, is defined by a Wigner coefficient, while the dependence on  $e$  is in terms of a Hansen coefficient. Both are defined and explained further in the appendices.

Taking the time average of this expansion for the torque picks out those terms whose phase is stationary, i.e. those terms for which the integers  $\ell$  and  $m$  are such that a linear

combination of the time  $t$  and the spin phase angle  $\gamma$ , is nearly constant over many orbits. Currently Mercury turns on its axis almost exactly  $3/2$  times per orbit, so that the terms with  $\ell=3$ ,  $m=-2$  or with  $\ell=-3$ ,  $m=2$  remain after long-term averaging.

It is meaningful therefore in the current situation to define the "stroboscopic phase angle"  $\gamma_0$  by

$$\gamma_0 \equiv \gamma - \frac{3}{2} \frac{2\pi t}{P}$$

where  $P$  is the period of Mercury's orbit. The differential equation governing the angle  $\gamma$ , shown above in schematic form, becomes after averaging

$$\frac{d^2 \gamma_0}{dt^2} = f(\gamma_0, \theta, \varphi, e, \Omega, i, \omega).$$

The function  $f$  here turns out to act essentially like  $-A \sin 2\gamma_0$  so that this equation is essentially a pendulum equation. One of the solutions to the pendulum equation is simple oscillation. This is believed to be the current behavior of  $\gamma_0$ . That is, assuming that  $\gamma_0$  oscillates around zero within a narrow amplitude, the number of rotations per orbital period that Mercury makes will similarly oscillate around  $3/2$ ,

Whenever the spin rate  $\frac{d\gamma}{dt}$  of Mercury is very nearly an integral or half-integral (since a  $Y_{\ell m}$  approximation through  $\ell=2$  is bilaterally symmetric) multiple of the mean orbital motion  $2\pi/P$ , it is meaningful to define a stroboscopic phase variable. The differential equation will average into a pendulum-like equation. The possibility exists therefore for the spin rate to be trapped at any number of resonant values. As will

be shown, the probability of being trapped in high-numbered resonances (such as the spin rate being three or more times the mean orbital motion) is quite small.

When the spin rate is between half-integral or integral values of the mean orbital motion, the differential equation for the spin phase angle time-averages into the simpler form

$$\frac{d^2\psi}{dt^2} = f\left(\frac{d\psi}{dt}, \theta, \varphi, e, \alpha, \iota, \omega\right)$$

The function  $f$  has a negative sign whenever the spin rate is high. The spin rate is therefore decelerated so long as it is above a threshold value. Depending on the model of elasticity chosen for the planet Mercury, the spin rate below which the function  $f$  changes to positive sign is generally between once and one and a half times per orbit. If no trapping in resonances occurs, then, the spin rate will come to rest at just this cross-over rate, for which the solar torque exerted on Mercury averages to zero in one orbit.



## Chapter II. The Mathematical Model

### The Two Torques

The Sun's gravitational field will be assumed to obey a perfect inverse square law.

However, Mercury is an extended body and so its limb nearest the Sun experiences a higher gravitational field than the farther limb. This difference, though minute, is sufficient to distort the surface shape of the planet. To a first approximation, we may say that this tidal force raises ~~two~~ bulges in the surface, one at the subsolar point and one antipodally opposite. As Mercury rotates on its axis and moves ahead in its orbit, the subsolar point moves. The bulges must therefore, "subside" and reform at the new subsolar point. However, the material comprising the planet is not perfectly elastic and the position of the bulges will lag or precede the subsolar point by a small angle. The Sun's gravitational field exerts a torque on these bulges since they do not lie along the straight line connecting the centers of Mercury and the Sun. This torque acts to slow down or speed up the rotation of the planet.

For a circular orbit, this tidal torque is zero when the planet spins exactly once per orbit. For a moderately elliptical orbit such as Mercury's, the equilibrium spin rate is about 1.3 times per orbit for one tidal model (Peale and Gold 1965), and between 1.0 and 1.5 times per orbit for other models.

A second torque is that of the Sun's gravitational field acting on the permanent asymmetries in the planet's shape. Mer-

cury can be modeled by a triaxial ellipsoid, spinning around its shortest axis. For the Moon, the axes differ in length by about 1 part in  $10^4$ . Mercury, a comparably sized body, is probably similar. An important difference from the tidal torque is that the asymmetry torque depends not only on the spin rate, but on the spin phase, as follows.

Define the solar spin phase angle as the spin phase angle (referred sidereally) minus the true anomaly  $f$  ( $f$  is the angle between the vector from Sun to perihelion and the vector from Sun to planet). Define also the mean motion  $n=2\pi/(\text{orbital period})$ , the mean anomaly  $M=n \cdot (\text{time} - \text{initial time})$  and  $\dot{\psi}$ =sidereal spin rate. Then the solar spin phase is  $\frac{\dot{\psi}M}{n} - f$ . For a circular orbit and a spin rate  $\dot{\psi}=n$ , that is, once per orbit, the solar spin phase will be identically zero and the Sun will appear fixed in position to an observer on the planet's surface. It is interesting to compute the solar spin phase for Mercury in its maximally eccentric orbit of  $e=.24$  for two different spin states,  $\dot{\psi}=n$  (one rotation per orbit) and  $\dot{\psi}=3n/2$  (one and a half rotations per orbit):

$f$	$\dot{f}$	$(a/r)^3$	$(a/r)^6$	$(\frac{3}{2})M-f$	$M-f$
$0^\circ$	$1.65n$	2.5	6.0	$0^\circ$	$0^\circ$
$30^\circ$	$1.58n$	2.1	4.4	$-3^\circ$	$17^\circ$
$60^\circ$	$1.35n$	1.7	2.8	$3^\circ$	$27^\circ$
$90^\circ$	$1.07n$	1.2	1.4	$21^\circ$	$25^\circ$
$135^\circ$	$.72n$	.7	.5	$50^\circ$	$14^\circ$
$180^\circ$	$.63n$	.5	.3	$90^\circ$	$0^\circ$

Table 1

The point  $f=0^\circ$  is perihelion.  $f$  is the orbital speed,  $a$  is the semi-major axis and  $r$  the distance from the Sun to Mercury at anomaly  $f$ . Models for the tidal and asymmetry torques (Counselman, 1969) predict they are proportional to  $(a/r)^3$  or  $(a/r)^6$ ; we see here how strong they are at perihelion. The  $\frac{3}{2}n$  resonance is well matched to the high orbital speeds around perihelion -- the phase angle varies only  $\pm 3^\circ$  as far away as  $60^\circ$  from perihelion. Therefore, in the  $\frac{3}{2}n$  resonance state, as Mercury is currently, only one face of the planet is presented to the Sun for a considerable portion of the orbit near perihelion.

The instantaneous asymmetry torque is proportional to the sine of twice the solar spin angle. Over one orbit, the asymmetry torque will therefore average to zero, unless the spin rate is an integral or half integral multiple of the mean motion (or very close to such a resonance). In those cases, the averaged asymmetry torque will be non-zero and will depend on the sine of  $2 \times$  the solar spin angle at perihelion; the latter angle is called the stroboscopic spin phase.

## The Long Slowdown

We do not know the rotation period of Mercury four billion years ago. However, most of the planets now have periods in the range 10 to 24 hours. Except for Venus and the Earth, whose spins are affected by the Earth and the Moon, respectively, no other planet is close enough to a body large enough to perturb its rotation. (Recall how rapidly applied torque decreases with distance--by at least the inverse cube.) The Sun can produce tidal effects large enough to alter Mercury's rotation. However the Sun's torques will not secularly alter Mercury's much larger orbital angular momentum. Planetary perturbations will also not secularly alter Mercury's semi-major axis (Brouwer and van Woerkom, 1950), and therefore, by Kepler's third law, not its mean motion  $n$  either. Hence, we may guess that Mercury's rotation period was originally about 20 hours, or  $100n$ . As almost all the planets do now, it probably rotated counterclockwise; it does so now. The original inclination of the spin axis from the orbit normal is unknown. Today, like most of the other planets, its inclination is small ( $< 10^\circ$ ). We picture the tidal torque as the primary agent in slowing the spin rate from perhaps  $100n$  down to the current  $1.5n$ . As discussed, however, the orbit period has not changed, and  $n$  is a constant. It will be shown below that the torque decelerates the spin rate by a factor of  $1/2$  in about  $10^8$  orbits. As the slowing spin rate passes through a resonance rate of  $(\frac{k}{2})n$  (for  $k =$  an integer), the asymmetry torque could average to a non-zero value and attempt to stabilize the spin rate. However, for high-numbered spin

resonances, the magnitude of the asymmetry torque is far less than that of the tidal torque (to be shown). Only for spin rates below about  $10n$  for Mercury (the threshold depends on the degree of asymmetry and on the eccentricity) is the asymmetry torque stronger than the tidal torque. However, capture at spin rate will be shown below to depend on the stroboscopic phase angle at the time the spin rate passes exactly through the resonance rate  $\frac{k}{2}n$ . Since we have no knowledge at all of the phase angle, we can only compute ranges within which the phase angle must be for capture to occur; i.e. we may compute the probability of capture at each resonance rate.

## The Coordinate Systems

Three sets of coordinates are important to torque calculation--the orbit plane system and two planetary systems. Define  $\hat{L}\hat{M}\hat{N}$  to be the inertial coordinate system, righthanded ( $\hat{N} = \hat{L} \times \hat{M}$ ) and orthonormal, as will be all systems that will be used. Define  $\hat{X}\hat{Y}\hat{Z}$  as the orbit plane system,  $\hat{Z}$  the orbit normal and  $\hat{X}$  pointing to perihelion. Define  $\hat{i}\hat{j}\hat{k}$  as a system fixed in the planet, pointing along the principal axes of inertia ( $\hat{k}$  is the spin axis). We rotate inertial coordinate axes into orbital coordinate axes by the usual Euler angles  $(\Omega, \iota, \omega)$  and from orbital to planetary axes by the Euler angles  $(\psi, \theta, \phi)$  (Fig. 2). Since we will later average out the rapidly changing spin angle  $\phi$ , we also define the planet-fixed, non-spinning coordinate axes  $\hat{\mu}\hat{\nu}\hat{\kappa}$  rotated from the  $\hat{X}\hat{Y}\hat{Z}$  axes by the Euler angles  $(\psi, \theta, 0)$ .

## The Torque Equation

For motion under torque as seen from an inertial coordinate system

$$\frac{d\mathbf{H}}{dt} = \mathbf{T}$$

where  $\mathbf{H}$  is the total angular momentum of the planet, and  $\mathbf{T}$  is the Sun's torque on it.

## The Angular Momentum

The angular momentum in an inertial coordinate system is

$$\mathbf{H} = \int_{\text{planet}} dm (\mathbf{r} + \mathbf{R}) \times \left( \frac{d\mathbf{r}}{dt} + \frac{d\mathbf{R}}{dt} \right)$$

where  $\mathbf{R}$  is the vector from the center of the sun to the center of mass of the planet, and  $\mathbf{r}$  is the vector from the center of

mass to the mass particle  $dm$ . Since

$$\int_{\text{planet}} dm \underline{r} = 0$$

it is easily shown that

$$\underline{H} = \int_{\text{planet}} dm \left( \underline{r} \times \frac{d\underline{r}}{dt} + \underline{R} \times \frac{d\underline{R}}{dt} \right)$$

the principal terms of which are

$$\underline{H} = C \dot{\psi} \hat{k} + M_{\text{planet}} R^2 \dot{f} \hat{z}$$

$M_{\text{planet}}$  is the mass of Mercury,  $\dot{f}$  is the orbital speed,  $\hat{k}$  the spin axis, and  $C$  is the principal moment of inertia.

Many more terms could be included here. On the one hand, we ignore precession of the orbitplane because it is very small ( $\dot{\Omega} < 10^{-8}$ /orbit) and on the other hand, we ignore the Chandler wobble of the spin axis, since it is damped rapidly compared to the time scales which are considered below. Finally, differentiating,

$$\begin{aligned} \frac{d\underline{H}}{dt} &= C \ddot{\psi} \hat{k} + C \dot{\psi} [\dot{\psi} \hat{z} + \dot{\theta} \hat{\mu} + \dot{\psi} \hat{k}] \times \hat{k} \\ &= C \ddot{\psi} \hat{k} + C \dot{\psi} \dot{\psi} \sin \theta \hat{\mu} - C \dot{\psi} \dot{\theta} \hat{z} \end{aligned}$$

(We have used a wellknown theorem about the derivative with time of a vector defined by Euler angles (Goldstein, 1950)). The orbital angular momentum is assumed constant to our degree of approximation and further neglected terms involve very small cross-terms, as  $\dot{\psi} \dot{\theta}$ , etc. The second term is the familiar precession  $\dot{\psi}$  of the spin axis; it vanishes when  $\theta$ , the axis inclination from the orbit normal, is zero. The third term concerns the changing tilt, and the first is the deceleration of the spin.

The precession of the spin axis is due principally to the

asymmetry torque. The change of inclination is due principally to the tidal torque. For a spherical planet in a circular orbit, it is very easy to show (see Qualitative Estimates, below) that the rate of change of inclination depends upon a factor  $\frac{1}{2} \dot{\psi} \cos \theta - n$ . Thus, for spin rates  $\dot{\psi}$  of more than  $2/\cos \theta$  turns per orbit, the inclination will increase. For spin rates less than this, which includes all rates  $< 2n$ , the inclination will decrease.

### The Torque

The force of the Sun on Mercury is the negative of Mercury's force on the Sun. We compute it therefore by

$$\underline{T}_{\text{Sun on Mercury}} = -M_{\odot} \underline{R} \times \underline{F}_{\text{Mercury on Sun}}$$

where  $\underline{R}$  is the vector from planet to Sun and  $\underline{F}$  is the force per unit mass.

We now define three important vectors; all are given by their spherical coordinates in the  $\hat{i}\hat{j}\hat{k}$  axes fixed in the planet, with origin at the planetary center of mass:

$$\underline{R} = (R, \Theta, \Phi) \text{ to the Sun.}$$

$$\underline{r}'' = (r'', \theta'', \varphi'') \text{ to an observation point in space}$$

$$\underline{r}' = (r', \theta', \varphi') \text{ to a mass element } dm' \text{ inside the planet}$$

The planet's shape is distorted tidally by the Sun's presence besides the permanent asymmetry. The potential per unit mass felt at  $\underline{r}''$  due to the planet is



$$U(\underline{r}''', \underline{R}) = - \int_{\text{planet, whose shape depends on } \underline{R}} dm' \frac{G}{|\underline{r}'' - \underline{r}'|}$$

Then the torque on the planet is, from the definition of torque above:

$$\underline{\Gamma} = - M_{\odot} \left\{ \underline{r}'' \times \left[ - \underline{\nabla} U(\underline{r}'', \underline{R}) \right] \right\}_{\underline{r}'' = \underline{R}}$$

where  $\underline{\nabla} = \frac{\partial}{\partial \underline{r}''}$

Re-expressing in terms of the well known operator

$$\underline{L} = -i \underline{r}'' \times \underline{\nabla}$$

$$\underline{\Gamma} = M_{\odot} [i \underline{L} U(\underline{r}'', \underline{R})]_{\underline{r}'' = \underline{R}}$$

Now expand the potential U in terms of the spherical harmonics  $Y_{\ell m}$ , since they are eigenfunctions of  $\underline{L}$  (see Jackson, 1962):

$$U(\underline{r}'', \underline{R}) = - \sum_{\ell=0}^{\infty} \sum_{m=-\ell}^{\ell} \frac{G}{r''^{\ell+1}} I_{\ell m}(\underline{R}) Y_{\ell m}(\theta'', \varphi'')$$

where the inertia coefficients

$$I_{\ell m}(\underline{R}) = \frac{4\pi}{2\ell+1} D_{\ell m} \int_{\text{planet}} dm' r'^{\ell} Y_{\ell m}^*(\theta', \varphi')$$

(planet shape depends on  $\underline{R}$ )

and  $D_{\ell m} = \sqrt{\frac{2\ell+1}{4\pi} \frac{(\ell-m)!}{(\ell+m)!}}$  . - 25 -

Inserting this expression into the torque formula and applying operator  $\underline{L}$  to the spherical harmonics according to well-known formulae (Jackson):

$$\underline{T} = \sum_{l=0}^{\infty} \sum_{m=-l}^l \sum_{s=-l}^{+l} \frac{GM_{\odot}}{R^{l+1}} I_{lm}(R) (-i)^s \underline{\lambda}_{lms} \exp(is\psi) Y_{l,ms}(\Theta, \Phi) / D_{l,ms}$$

where:

$$\underline{\lambda}_{lms} = -im\hat{k} \delta_{s0} + \left( \frac{\hat{\mu} - i\hat{\nu}}{2} \right) \delta_{s1} + (l+m)(l+1-m) \left( \frac{-\hat{\mu} - i\hat{\nu}}{2} \right) \delta_{s,-1}$$

given in terms of the equatorial, but non-rotating, coordinate axes  $\hat{\mu}\hat{\nu}\hat{k}$ ; the Kronecker delta symbol is defined by

$$\delta_{st} = \begin{cases} 1, & s=t \\ 0, & s \neq t \end{cases}$$

This formula for the torque is unsatisfactory for further calculation until high-frequency terms in it are averaged out. Specifically, the factor  $\exp(is\psi)$  depends upon the quickly changing spin phase angle  $\psi$ ; and both the inertia coefficients and the spherical harmonics depend upon  $\underline{R}$ , the position vector of the Sun in its orbit.

## The Inertia Coefficients

First, we give the inertia coefficients in an explicit form. Following App. D, we split the integral for  $I_{em}(\underline{R})$  into two parts: that over the permanent shape of the planet and that over the tidal distortions. This correspondingly splits up the torque into the two kinds discussed in the introductory chapter. Thus:

$$I_{em}(\underline{R}) = I_{em}^{(1)} + I_{em}^{(2)}(\underline{R})$$

and correspondingly,

$$\underline{T} = \underline{T}^{(1)} + \underline{T}^{(2)}$$

Superscript 1 refers to permanent asymmetry, 2 to tidal effects.

The permanent part of the inertia coefficients is, from (D.6)

$$I_{em}^{(1)} = M_{\text{planet}} \delta_{l0} \delta_{m0} + \delta_{l2} \left[ -\gamma C \delta_{m0} + \frac{\beta C}{8} \delta_{m1} + 3\beta C \delta_{m,-1} \right]$$

where the flattening

$$\gamma = 1 - \frac{A+B}{2C}$$

and the deviation from equatorial circularity

$$\beta = \frac{B-A}{C}$$

A, B, and C being the principal moments of inertia. Therefore, the asymmetry torque  $\underline{T}^{(1)}$  depends only on A, B, and C; in fact, it can be shown to be just

$$\underline{T}^{(1)} = M_{\oplus} i \underline{L} U_{\text{MacCullagh}}$$

where  $U_{\text{MacCullagh}}$  is MacCullagh's potential for an ellipsoidal planet (Danby, 1962 and (D.10) below).

Terms past  $\lambda = 2$  are not taken because the factor  $I_{\lambda m} / R^{\lambda+1}$  in the torque is proportional approximately to the  $\lambda$ 'th power of the ratio of the planetary radius to the distance from the Sun, which is, of course, quite small.  $\beta$  and  $\gamma$  for the Moon, a body comparable in size and spin rate to Mercury, are about  $10^{-4}$ .

The computation of the inertia due to the tidal distortions follows Counselman (1967), who in turn, follows Love's development. The Sun is taken to be spherical and its potential expanded in spherical harmonics around Mercury's center of mass. Following Love's treatment, the  $\lambda$ 'th term gives rise to a similar term in the expansion of the planet's potential, identical except for a dimensionless multiplicative factor  $k_\lambda$ , the Love number, a divisor  $g$ , the planet's surface gravity, and a small "lag" angle of the tidal "bulge" relative to the subsolar point. From eq. (D.12), the tidal-induced inertia is:

$$I_{\lambda m}^{(2)}(R) = \alpha C a^3 \int_{\Omega_2} \frac{(l-m)!}{(l+m)!} [R^{-\lambda+1} Y_{\lambda m}^*(\Theta, \Phi) / D_{\lambda m}] \text{lagging}$$

where  $a$  is the semimajor axis of the orbit and

$$\alpha = k_2 \frac{n^2}{\omega_0^2}$$

where  $n$  is the mean motion =  $2\pi /$  period of orbit, and  $\omega_0$  is the mean motion of a "rooftop satellite" around the planet, i.e. one which skims the surface. The ratio  $n/\omega_0 < 10^{-3}$  for Mercury.

### Chapter III. Time Averaging and Elasticity Models

Magnitude of terms. Since the torque equation is impossible to solve analytically, we shall make several approximations. It is important therefore to know the magnitude of our variables.

Variables observed astronomically:

$n$ , the mean motion, is  $2\pi/88 \text{ day}^{-1}$ .

$e$ , the eccentricity, is currently .2 and varies from .12 to .24.

$\dot{\psi}$ , the spin rate, is  $1.5n$ , i.e. 1.5 times per orbit, or a period of 59 days.

$\theta$ , the inclination, is probably less than  $10^\circ$  now.

$L$ , the inclination of the orbit, is not relevant here: it is  $7^\circ$  from the earth's ecliptic.

$\dot{i}$  is  $1.2 \times 10^{-8}n$ , i.e. a period of 20 million years.

$\dot{\omega}$  is  $2.5 \times 10^{-6}n$ , i.e. a period of 100,000 years.

$\dot{s}$  is  $-1.3 \times 10^{-6}n$ , i.e. a period of 180,000 years.

$\omega_c$  is  $2\pi/90 \text{ min}^{-1}$ , the same as for the Earth.

The above values are taken from Allen (1964) or Brouwer and Van Woerkom (1950).

$\alpha$  is  $k_2(n/\omega_c)^2 = 5 \times 10^{-7}k_2$  and  $k_2 = .3$  for the Earth; so  $\alpha = 10^{-8}$  for Mercury.

$\beta$  is  $10^{-4}$  for the Moon, which is the same diameter as Mercury, since the density of Mercury is almost twice that of the Moon, this might be a rough upper limit. The capture probabilities (for one elasticity model, at least) depend strongly on  $\beta$ .

$\gamma$  for Mercury in hydrostasis, would be approximately the square of the ratio of the rotation velocity over the escape velocity.

Mercury and Earth have a similar density, the Earth's flattening is  $1/297$  and Mercury's spin  $\psi$  is  $1/60$  the Earth's; so Mercury's  $\gamma > 10^{-6}$ . More likely it is about  $10^{-4}$ , comparable to the axial asymmetry  $\beta$ .

These values are taken from Counselman (1967 and private communication).

### Time Averaging

Two important difficulties are now solved by averaging over a period of many orbits. First, both torques depend instantaneously upon short term orbital and spin motion. Secondly, there is no way to try different models for tidal lag in the tidal inertia coefficients until they are explicitly made functions of time, rather than implicitly through the Sun vector R.

Hence we should convert the Sun vector R from dependence upon spherical coordinates to dependence upon the Keplerian orbit parameters -- principally  $a$ , the semimajor orbit axis,  $e$ , the orbit eccentricity,  $\theta$ , the inclination of the orbit plane from the equatorial plane, and  $M$ , the mean anomaly =  $n(t - t_0)$ , where  $t - t_0$  is the time from some starting point. Along with the conversion of R, the spherical harmonics must also be changed.

This formidable piece of algebra is accomplished in Appendices A, B and C. The Hansen functions of the eccentricity  $G_{\lambda pq}(e)$  and the inclination polynomials of the tilt  $F_{\lambda mp}(\theta)$  are defined and derived therein. Combining Eqs. (B. 5) and (C.10):

$$R^{-l-1} Y_{lm}(\Theta, \Phi) / D_{lm} = a^{-l-1} i^{l+m} \sum_{p=0}^l \sum_{q=-\infty}^{\infty} F_{lmp}(\theta) G_{lpq}(e) \exp(i V_{lmpq})$$

where the overall phase angle:

$$V_{lmpq} = (l-2p+q) M - m \psi - (l-2p)\varphi$$

depends on the spin phase angle  $\psi$  and the spin axis precession angle  $\varphi$ .

For order of magnitude estimates, the  $F_{lmp}(\theta)$  are of order:  $\theta^{|l-2p-m|}$  for small  $\theta$  and of order 1 for  $\theta$  near  $\pi/2$ , while the  $G_{lpq}(e)$  are of order  $e^{|q|}$ . Since even for Mercury, the eccentricity  $e$  is never more than 0.24, the terms of the above series decline quite rapidly away from  $q = 0$ .

Next, the lag angles are introduced by writing

$$[R^{-l-1} Y_{lm}(\Theta, \Phi) / D_{lm}]_{\text{lagging}} = a^{-l-1} i^{l+m} \sum_{p,q} F_{lmp}(\theta) G_{lpq}(e) \exp(i V_{lmpq} - i \epsilon_{lmpq})$$

Many different physical models for tidal inelasticity may be modeled by altering the lag angles  $\epsilon_{lmpq}$ . However, one consistency relationship must be satisfied for all models. Since the tidal bulges lag the subsolar point when the spin rate  $\dot{\psi}$  is less than the orbital rate  $\dot{M} = n$ , and precede it for the reverse case, the  $\epsilon_{lmpq}$  must have the same sign as the compound frequency  $\dot{V}_{lmpq}$ . Inserting our conversion formula into its equations for torque and for inertia coefficients, we time average over one orbit:

$$\langle I \rangle_M = \frac{1}{2\pi} \int_0^{2\pi} dM \underline{I}$$

In particular, it is necessary to define a new variable, the stroboscopic spin phase angle  $\psi_0$ , for those times when the spin rate is very nearly a half integer multiple of  $n$ . For

when it is, then:

$$\langle \exp(i\nu_{\text{LMP}}\psi_0) \rangle_M = \begin{cases} \exp(-im\psi_0 - i(l-2p)\psi), & m\dot{\psi} = (l-2p+q)n \\ 0, & \text{otherwise} \end{cases}$$

$\psi_0$  is defined as the phase angle  $\psi$  seen at perihelion, exactly as discussed above. The rate of change of the stroboscopic spin angle,  $\dot{\psi}_0$ , will be shown below to be quite slow for large spin rate  $\dot{\psi}$  near resonance, so slow that the precession angle  $\psi$  will change rapidly compared to  $\psi_0$  and may therefore be averaged out. At low spin-rates, such as below  $4n$  for Mercury,  $\dot{\psi}_0$  will be seen to be comparable to or larger than  $\dot{\psi}$ , so that  $\psi$  will be effectively constant during a resonance passage. The capture probability turns out in fact to be higher for  $\psi = 90^\circ$  than  $\psi = 0^\circ$ ; that is, capture is more likely when the spin axis has a vector component pointing  $90^\circ$  away from perihelion and from the orbit normal.

### Averaged Asymmetry Torque

To make our variables dimensionless, we adopt the convention that

$$X' = \frac{dx}{dM} = \frac{\dot{x}}{n}$$

and divide the torques by  $n^2C$ . Then, the asymmetry torque averaged over one orbit becomes

$$\begin{aligned} \frac{1}{n^2C} \langle T^{(1)} \rangle_M &= \gamma \sum_{p=0}^2 F_{21p}(\theta) G_{2,p,2p-2}(e) \left[ \hat{\mu} \cos(2p-2)\psi + \hat{\nu} \sin(2p-2)\psi \right] \\ &\quad - \frac{\beta}{2} \sum_{p=0}^2 G_{2,p,2(\gamma'+p-1)}(e) \left\{ F_{22p}(\theta) \sin[2\psi_0 - 2(p-1)\psi] \hat{k} + \right. \\ &\quad \left. + F_{21p}(\theta) \left( \hat{\mu} \cos[2\psi_0 - 2(p-1)\psi] + \hat{\nu} \sin[2\psi_0 - 2(p-1)\psi] \right) \right\} \end{aligned}$$



At high spin rates, when  $\psi$  also can be averaged out, only the term for  $p = 1$  survives the second averaging:

$$\frac{1}{n^2 C} \langle \underline{T}^{(1)} \rangle_{M\varphi} = \gamma F_{211}(\theta) G_{210}(e) \hat{\mu} - \frac{\beta}{2} G_{2,1,2\psi'}(e) \left\{ F_{221}(\theta) \sin 2\psi_0 \hat{k} + F_{211}(\theta) [\hat{\mu} \cos 2\psi_0 + \hat{z} \sin 2\psi_0] \right\}$$

For reference,

$$F_{211}(\theta) = -\frac{3}{4} \sin 2\theta$$

$$F_{221}(\theta) = \frac{3}{2} \sin^2 \theta$$

$$G_{210}(e) = (1-e^2)^{-3/2}$$

and  $G_{2,1,2\psi'}(e)$  is of the order  $e^{12\psi'}$ . The  $\gamma$  term is the well-known solar precession torque. The  $\beta$  term vanishes if the spin rate  $\psi'$  is not very close to a half integer, or if  $\beta = 0$  (the equatorial profile is circular) or if the eccentricity  $e$  of the orbit vanishes. These agree with our intuitive feel for the asymmetry torque from above. Also, as noted above, the asymmetry torque depends upon the stroboscopic phase angle  $\psi_0$ . Again note the extreme smallness of the  $\beta$  term for high spin rate, as it is of order  $e^{12\psi'}$ .

### Averaged Tidal Torque

Similarly, the tidal torque averaged over time is:

$$\frac{1}{n^2 C} \langle \underline{T}^{(2)} \rangle_M = \alpha \sum_{m=0}^2 \sum_{s=1}^1 \sum_{p=0}^2 \sum_{q=0}^{\infty} \frac{(2-m)!}{(2+m)!} F_{2,mts,\theta}(\theta) F_{2mp}(\theta) G_{2pq}(e) \times G_{2PQ}(e) \exp [i \epsilon_{2mpq} + i 2(\beta - P)\varphi] \underline{\lambda}_{2ms}$$

where  $Q = q + 2p - 2P$ . Further, averaging over  $\varphi$  and rearranging,

$$\frac{1}{h^2 C} \langle T^{(2)} \rangle_{M\psi} = \alpha \sum_{m \leq p \leq q} \frac{(2-m)!}{(2+m)!} F_{2,m+p}(\theta) F_{2mp}(\theta) [G_{2pq}(e)]^2 \times$$

$$\times \left\{ \hat{\mu} [\delta_{s_1} - (2+m)(3-m)(1-\delta_{s_0})\delta_{s,-1}] \cos \epsilon_{2mpq} + [2m\delta_{s_0} \hat{k} + (\delta_{s_1} + (2+m)(3-m)(1-\delta_{m0})\delta_{s,-1})] \Delta m \epsilon_{2mpq} \right\}$$

The principal term which affects the spin rate  $\gamma'$  is the  $\hat{k}$  component. The  $\hat{\mu}$  component affecting precession is negligible compared to the  $\gamma$  term above, since  $\alpha \ll \gamma$ . The  $\hat{v}$  component is the principal term affecting the inclination. We will ignore the asymmetry  $\hat{v}$  component since passage through resonance does not permanently affect  $\theta$  (as if, for example,  $\theta$  were captured into a resonance).

### Qualitative Changes in Time

Hence, writing explicitly the equations of motion for the variable spin rate  $\gamma'$ , precession angle  $\varphi$  and inclination  $\theta$ :

$$\gamma'' = \alpha \sum_{m=0}^2 \sum_{p=0}^2 \sum_{q=-\infty}^{\infty} \frac{(2-m)!}{(2+m)!} [F_{2mp}(\theta) G_{2pq}(e)]^2 2m \Delta m \epsilon_{2mpq} - \frac{\beta}{2} F_{221}(\theta) G_{2,2\gamma'}(e) \sin 2\psi_0$$

$$\varphi' = \frac{3}{2} \gamma \frac{\cos \theta}{\gamma' (1-e^2)^{3/2}}$$

$$\theta' = \frac{\alpha}{\gamma'} \sum_{mpq} \frac{(2-m)!}{(2+m)!} [G_{2pq}(e)]^2 [F_{2,m+p}(\theta) + (2+m)(3-m)(1-\delta_{m0})F_{2,m-1,p}(\theta)] \Delta m \epsilon_{2mpq}$$

From these equations we can get a feel for the behavior of  $\gamma'$ ,  $\varphi$  and  $\theta$  in time. Since  $\epsilon_{2mpq}$  has the sign of :

$$\dot{V}_{2mpq} = (2-2p+q) \dot{n} - m \dot{\gamma}' - (2-2p) \dot{\varphi} < 0$$

for large  $\gamma'$ ,  $\gamma''$  will be negative; thus, between resonance values, when the  $\beta$  term averages to zero,  $\gamma'$  decreases monotonically.

Since  $\epsilon_{2mpq}$  is small, we let  $\sin \epsilon \approx \epsilon$ . Then  $\psi''$  is of the order  $\propto \epsilon$  which is  $< 0$ . The sign of  $\psi''$  changes to positive for the equilibrium spin rate between  $1.0n$  and  $1.5n$  as expected for an elliptical orbit.

As mentioned above,  $\theta'$  is positive for spin rates higher than about  $3n$ , and negative below this. In the long deceleration from an assumed primeval spin rate of perhaps  $100n$  (i.e. a rotation period of 20 hours), the inclination increased; numerical integration will show that it can increase to a maximum near  $60^\circ$  at  $3n$ , for almost any small initial inclination. As the spin rate drops below  $3n$ , the inclination rapidly decreases again. However, since the inclination may well have been large for the spin rate in the critical region of  $3n$  to  $1.5n$ , we must examine the inclination's effect on capture probabilities.

$\psi'$  is always positive and varies mainly with the spin rate. The precession of the spin axis around the orbit normal is therefore fairly steady.

### Models for Phase Lag

The quality factor  $Q$  (not to be confused with subscript  $Q$  above) for a sinusoidally stressed elastic system is defined:

$$Q = \frac{2\pi E_{\max}}{\Delta E}$$

where  $E_{\max}$  is the peak stored elastic energy and  $\Delta E$  is the energy dissipated per cycle of the strain oscillation. The larger the quality factor, the more elastic the system is.

In linear systems, the response to a sinusoidal driving force is sinusoidal with a phase lag angle independent of the driving amplitude but dependent, in general, upon the driving frequency. This phase lag angle  $\epsilon$  is related to the  $Q$  of the system by

$$\tan \epsilon = \frac{1}{Q}$$

In general,  $Q$  is a function of frequency for a linear system. For a nearly-elastic, high  $Q$  system with slight viscous velocity damping,  $Q$  is inversely proportional to frequency, so that  $\epsilon$  is proportional to frequency. This behavior of  $\epsilon$  vs. frequency corresponds to constant time lag of the response with respect to the driving force. Such a model is 1) the viscous model:

$$\tan \epsilon_{\text{emp}} = \frac{1}{Q} = \frac{1}{Q_0} v'_{\text{emp}} = \frac{1}{Q_0} [l-2p+q - m\eta' - (l-2p)\eta']$$

Another linear phase-lag model that should be considered is one for which  $Q$  and  $\epsilon$  are independent of frequency.

$Q$  has been measured for many terrestrial rocks over a wide range of driving frequencies (Knopoff & MacDonald, 1960). From about  $10^{-2}$ Hz to over  $10^8$ Hz for most rocks,  $Q$  is more or less constant, with about a logarithmic decrease for increasing frequency. Although this is suggestive, for the extremely low frequencies encountered in celestial torques ( $10^{-6}$ Hz for Mercury), we must resort to theoretical justification based on models of inelastic mechanisms (Knopoff & MacDonald, 1960; Lomnitz, 1957). They suggest that the constant  $Q$  approximation is true even at these low frequencies.

Following Lomnitz, we define a model in which  $Q$ , and hence  $\epsilon$ , depends only on the sign of the driving frequency\*; such a model is 2) the step model:

$$\tan \epsilon_{\text{empq}} = \frac{1}{Q} = \frac{1}{Q_0} \text{sign}(v'_{\text{empq}}) = \frac{1}{Q_0} \text{sign} [l-2p+q - m\gamma' - (l-2p)\varphi].$$

More important than the general shape of  $Q$  vs. frequency is how the phase lag changes direction when the sign of the driving frequency changes. For in the equations above on p. 33 for the tidal torque, the driving frequency is  $v'_{\text{mpq}}$ , whose magnitude is largely determined by the subscript  $q$ . Since  $q$  is the multiplier for the overtone of the basic orbital frequency, it can grow indefinitely large. However, the factor  $[G_{\text{mpq}}(e)]^2$  in the tidal torque formula decreases rapidly for  $|q|$  large. Furthermore, we saw that the phenomenon of capture depends strongly on the component of the tidal torque that changes sign with  $\dot{\gamma}_0$ , that is, the term in the series for which the compound driving frequency  $v'_{\text{mpq}}$  is 0 at the particular resonance.

From Goldreich & Soter (1966),  $Q$  for Mercury is no more than 190 and is probably not much smaller. Hence the phase lag is small and we may approximate the  $\tan \epsilon$  and  $\sin \epsilon$  by  $\epsilon$ .

\*Strictly speaking,  $Q$  is unsigned and is what we call here  $Q_0$ .

## Chapter IV. Resonance Capture

As the spin rate passes from just above a half-integral multiple of  $n$  to just below, the  $\beta$  asymmetry torque term in  $\dot{\gamma}^u$  averages to a non-zero value and begins to affect the spin rate. Since it is proportional to the sine of the stroboscopic spin angle  $\gamma_0$ , and so is typically much larger ( $\beta \gg \alpha$ ) in magnitude than the  $\alpha$  tidal torque term, the equation for  $\dot{\gamma}^u$  becomes just the equation of motion of a two headed pendulum with frictional pivot.

To make this clear, take a series of stroboscopic "photographs" of the planet as it passes through perihelion on successive orbits. We assume the tilt is zero, that we are over the north pole, and that the Sun is at the bottom of figure 2.

The rotation is counterclockwise and the spin rate is just above the resonance rate; i.e.

$$\dot{\gamma} > \frac{k}{2} n$$

so the stroboscopic rate

$$\dot{\gamma}_0 = \dot{\gamma} - \frac{k}{2} n > 0$$

It is clear that in figures 2a and 2e, the Sun is exerting a counterclockwise asymmetry torque to speed up the rotation; in figure 2c it is slowing the rotation and in figures 2b and 2d, there is no torque.

However, the tidal torque, though much weaker, is always opposing the rotation. More precisely, overall it has the sign of

$$\dot{V}_{2m\beta\gamma} = (2-2\beta+\gamma - \frac{km}{z})n - m\dot{\gamma}_0$$

which is the sum of two subtorques, the first with constant negative sign, and the second with sign opposite to  $\dot{\gamma}_0$ , the speed of the stroboscopic phase angle.

The planet as seen stroboscopically will turn around and around for perhaps hundreds or thousands of orbits until the stroboscopic spin rate is just barely positive. The planet will then make one last turn and the asymmetry torque, acting like a friction pivot will bring the planet to a halt as in figure 2c or 2d. Now  $\dot{\gamma}_0$  turns negative and the planet will follow either figure 3 or 4.

As shown in figure 3, the end of the planet "rolls back down the hill" and over the top on the left side and escapes. Now  $\dot{\gamma}_0$  can only speed up in the negative direction, with the tidal torque acting mainly as a negative force.

However, as mentioned above, the tidal torque for  $\dot{\gamma}_0 < 0$  has a smaller magnitude than for  $\dot{\gamma}_0 > 0$ . By conservation of energy alone, the planet would "roll" from figure 4a to only figure 4c, symmetrically opposite the Sun-center line. The tidal torque, acting clockwise pushes the planet to 4d, which however is not over the "lip of the hill". The planet then rolls back as in figures 4d-g and repeats figure 4 endlessly (or rather with gradually decreasing amplitude, like a pendulum coming to rest). This is called resonance capture and figure 4 exhibits libration.

The difference between resonance capture and escape is thus seen to be the value of  $\psi_0$  at the exact instant that  $\dot{\psi}_0 = 0$ . In figure 3a,  $\psi_0$  is seen to be high enough on the right so that the roll back is to an equally high point on the left. The tidal torque then can push the planet over the edge.

Hence, the probability of capture is related to that range of  $\psi_0$  on either side of  $\psi_0 = 0$  within which the planet may stop when  $\dot{\psi}_0 = 0$  and be captured.

#### Capture Probability

While turning through an angle of  $\pi$  on the last forward roll, the planet loses a certain amount of its rotational kinetic energy to the tidal dissipation. There is a maximum energy  $E_{\max}$  that can be dissipated in a roll from  $\psi_0 = -\pi/2$  to  $\pi/2$ . Thus, the planet can have no more than  $E_{\max}$  energy at the beginning of the last roll or else it will roll further than  $\psi_0 = \pi/2$  and this will not be the last roll after all.

If on entering the last roll, the planet has  $\delta$  energy where  $\delta$  is much smaller than  $E_{\max}$ , the maximum roll forward will be to only a little farther than  $\psi_0 = 0$  and capture will occur, as in figure 4a. There is a maximum value  $\delta_{\max}$  that the planet can enter the last roll with and still be captured.

Since the actual energy  $\delta$  the planet will have is random, though it must be less than  $E_{\max}$ , and since only if  $\delta$  is less than  $\delta_{\max}$  will capture occur, it is reasonable to



define the capture probability as (Counselman, 1967)

$$P_{\text{capture}} = \frac{\delta_{\text{max}}}{E_{\text{max}}}$$

In the equation for  $\gamma''$ , replace the tidal torque term

by

$$\alpha [T_0 + T_1(\gamma_0')]$$

where  $T_1(\gamma_0')$  has the same sign as  $\gamma_0'$ . Then

$$\gamma_0'' = \gamma'' = \alpha [T_0 + T_1(\gamma_0')] - \frac{\beta}{2} F_{221}(\theta) G_{2,1,2\gamma_0'}(e) \sin 2\gamma_0$$

Integrating,

$$\frac{1}{2} \gamma_0'^2 - \frac{\beta}{4} F_{221}(\theta) G_{2,1,2\gamma_0'}(e) \cos 2\gamma_0 = \int \alpha [T_0 + T_1(\gamma_0')] d\gamma_0$$

that is, the kinetic plus the potential energy equals a constant which decreases slowly as  $\gamma_0'$  increases.

On the last roll, the right-hand side is virtually  $\frac{\beta}{4}$  and a good approximation to the motion is:

$$\gamma_0' = \left[ \beta F_{221}(\theta) G_{2,1,2\gamma_0'}(e) \right]^{1/2} \cos \gamma_0$$

We see that the magnitude of the right-hand side, which is the speed of the stroboscopic phase when the spin rate is near a resonance, is large for small spin rates and small for large rates.

The motion of the planet in the last roll may be seen in figure 5, a phase space diagram of  $\gamma_0'$  versus the "kinetic energy"  $\gamma_0'^2$ .

The periodic variations in  $\gamma_0'^2$  are caused by

$$\frac{\beta}{2} F_{221}(\theta) G_{2,1,2\gamma_0'}(e) \cos 2\gamma_0$$

while the slope, greatly exaggerated, is the loss to the tidal torque

$$\alpha \int [T_0 + T_1(\gamma_0')] d\gamma_0$$

The decrease in energy on the last roll, from  $\psi_0 = -\pi/2$  to  $\pi/2$ , is just the  $E_{\max}$  discussed above:

$$E_{\max} = \int_{-\pi/2}^{\pi/2} \alpha [T_0 + T_1(\psi_0')] d\psi_0$$

The maximum energy  $\delta_{\max}$  that the planet can have is the energy dissipated on the forward part of the last roll less the energy gained on the reverse roll:

$$\delta_{\max} = E_{\max} - \int_{+\pi/2}^{-\pi/2} \alpha [T_0 + T_1(\psi_0')] d\psi_0 = 2\alpha \int_{-\pi/2}^{\pi/2} T_1(\psi_0') \Big|_{\psi_0' > 0} d\psi_0$$

Performing the integrations using the approximation for  $\psi_0'$  given on p.41, we find the probability coefficients for the two models are:

$$P_{\text{capture}} = \frac{2 \sum_{mpq} B_{2mpq}}{\sum_{mpq} B_{2mpq} \left[ m - \frac{\pi}{2\sqrt{\beta FG}} ((2-2p)(1-\psi') + q - \frac{mk}{2}) \right]}$$

for the viscous model

$$P_{\text{capture}} = \frac{2 \sum_{mp} B_{2,m,p,2p-2+mk/2}}{\sum_{mpq} B_{2mpq} \text{sign} \left[ (2-2p)(1-\psi') - q + \frac{mk}{2} + m\sqrt{\beta FG} \right]}$$

for the step model

where the resonance is at  $\dot{\psi} = \frac{k}{2} n$  and the abbreviations

$$B_{2mpq} = m \frac{(2-m)!}{(2+m)!} [F_{2mp}(\theta) G_{2pq}(e)]^2$$

$$\sqrt{\beta FG} = \begin{cases} \sqrt{\beta F_{221}(\theta) G_{2,1,2\pi}(e)}, & \varphi \text{ averaged out} \\ \sqrt{\beta F_{220}(\theta) G_{2,1,2\pi,2}(e)}, & \varphi \text{ not averaged out} \end{cases}$$

The probability capture formula may be written in the following form:

$$P_{\text{capture}} = \frac{2S}{T_r},$$

where  $S$  is the sum of all the terms in the  $\hat{k}$  component of the tidal torque which change sign at this resonance, and  $T_r$  is the total value of the tidal torque at a spin rate just higher than the resonance value. This formula is very useful for the qualitative estimates that we make in the next section.

For reference, we give a short table of the  $F_{2mp}$  functions needed in the probability formulas (cf. table B.1):

$$F_{210}(\theta) = \frac{3}{4} (1 + \cos\theta) \sin\theta$$

$$F_{220}(\theta) = \frac{3}{4} (1 + \cos\theta)^2$$

$$F_{221}(\theta) = \frac{3}{2} \sin^2\theta$$

Note that the probability of capture is directly proportional to  $\sqrt{\beta}$  for the viscous model; that is, for this model, larger equatorial asymmetry means higher likelihood of capture.

## Chapter V Discussion of Results

### Qualitative Estimates

Before examining the computer-produced graphs of spin evolution and resonance capture probabilities, let us make "back of the envelope" qualitative estimates of the torques.

The tidal torque may be modelled as the torque exerted by the tidal bulges on the Sun. The bulges are approximately at the subsolar and antipodal points on the planet. For simplicity, let the planet be spherical and the orbit be circular.

Let  $\hat{r}(t)$  be the unit vector from the Sun to the center of the planet and  $\hat{R}(t)$  the unit vector from the Sun to the center of the planet to the subsolar bulge. At time  $t_0$ , let there be no bulges. Then  $\hat{R}(t_0) = -\hat{r}(t_0)$ . The tidal bulges then appear instantaneously. A very short time later, at  $t_1 = t_0 + t'$ , the bulges have been carried with the planet in two directions: along the orbital plane an angular distance  $\delta(t')$ , and along the equatorial plane an angular distance  $\Delta(t')$ .

We have

$$\hat{r}(t_1) = \hat{r}(t_0) \cos \delta + \hat{z} \times \hat{r}(t_0) \sin \delta$$
$$\hat{R}(t_1) = \hat{R}(t_0) \cos \Delta + \hat{k} \times \hat{R}(t_0) \sin \Delta + \hat{k} \cdot \hat{R}(t_0) \hat{k} (1 - \cos \Delta)$$

The gravitational attraction of the sunward bulge for the sun is proportional to

$$F_1 \propto \frac{\hat{r}(t_1) + \hat{R}(t_1)}{r^2}$$

while that of the antipodal bulge is

$$\underline{F}_2 \propto \frac{\hat{r}(t_1) - \hat{R}(t_1)}{(r+2R)^2}$$

Hence the torque of the bulges on the Sun is given proportionally by

$$\underline{T} \propto \hat{r}(t_1) \times [\underline{F}_1 + \underline{F}_2] = \frac{R(1-\frac{3R}{r})}{r^3} \hat{r}(t_1) \times \hat{R}(t_1)$$

Averaging over one orbit to eliminate  $t_0$  and  $t_1$ :

$$\begin{aligned} \langle \hat{r} \times \hat{R} \rangle &= -\hat{k} \left[ \sin(\Delta\delta) \left( \frac{1+\cos^2\theta}{2} \right) + \cos\Delta \sin\delta \frac{(1-\cos\theta)^2}{2} \right] \\ &\quad - \hat{i} \sin\theta \left[ \frac{1}{2} \sin\Delta \sin\delta - \cos\delta (1-\cos\Delta) \frac{\cos\theta}{2} \right] \\ &\quad - \hat{j} \sin\theta \left[ \sin\Delta \cos\delta \frac{\cos\theta}{2} - \sin\delta \left( \frac{1+\cos\Delta}{2} \right) \right] \end{aligned}$$

The viscous model above predicts that  $\Delta(t') = \dot{\psi} t'$  and  $\delta(t') = n t'$ , where  $t'$  is the displacement in time of the lagging bulges. The  $\hat{k}$  component gives the spin deceleration

$$\ddot{\psi} \propto -(\dot{\psi} - n) \left( \frac{1+\cos^2\theta}{2} \right) - n \frac{(1-\cos\theta)^2}{2}$$

while the  $\hat{j}$  component gives the tilt rate

$$\dot{\theta} \propto -\sin\theta \left[ \dot{\psi} \frac{\cos\theta}{2} - n \right]$$

The asymmetry torque must be modelled on a non-spherical planet in an elliptical orbit. By averaging the torque pictorially, the main characteristics are brought out. Fig. 2 shows the planet in several characteristic orientations. In Fig. 2b and 2d, the instantaneous torque is positive, since it will cause a counterclockwise motion. In Fig. 2c, the instantaneous torque is negative.

In Fig. 6, the planet is turning through one complete orbit at a rate of exactly  $3n$ . At perihelion, the stroboscopic

phase angle is set to zero. The orbit is divided into sectors of positive and negative instantaneous torque, as indicated by the arrow marking one end of the ellipsoidal planet. The spin axis is perpendicular to the orbital plane. It is clearly seen that the averaged asymmetry torque over one orbit is zero when the stroboscopic phase angle at perihelion is zero.

In Fig. 7, the stroboscopic phase at perihelion is set slightly negative (using the angle convention of Fig. 2). The narrow sector of positive torque at perihelion is sufficient to make the orbit-averaged torque also positive, since the torque is so strong at perihelion (Table 1).

To determine the effects of axis tilt, we project the arrow representing the planet's longest axis onto the orbital plane. When the tilt is zero, this arrow turns at a constant rate, as in Fig. 6 and 7. When the spin axis is tilted, the head of the arrow no longer traces a circle in the orbital plane, but an ellipse. Fig. 8a shows the path when the spin axis is perpendicular to the paper, Fig. 8b when it is tilted downward.

The projected phase angle is

$$\cos \psi_{\text{projected}} = \cos \psi \cos \theta [1 - \sin^2 \theta \cos^2 \psi]^{-1/2}$$

where  $\theta$  is the tilt. Then the derivatives

$$\frac{\dot{\psi}_{\text{projected}}}{\dot{\psi}} = \cos \theta [1 - \sin^2 \theta \cos^2 \psi]^{-1} = \begin{cases} > 1, & \psi = 0 \text{ or } \pi \\ < 1, & \psi = \frac{\pi}{2} \text{ or } \frac{3\pi}{2} \end{cases}$$

Thus if the spin axis is tilted toward the Sun in Fig. 7, the projected phase angle moves more quickly than for no inclination, the sector of positive torque is narrowed and the averaged torque decreases. The averaged torque increases if the spin axis points perpendicularly to the Sun-perihelion vector. Compare with the equations on p.32-3 where  $\psi$  is the precession angle just discussed.

Evolution by numerical integration.

Since the equations of motion of our model (p.34) are impossible to solve analytically, even with the simplifications we have made, we shall integrate them numerically. We shall gain a physical feel for our results if we first present plots of the averaged tidal torque, as a function of axis inclination  $\theta$  and spin rate  $\dot{\gamma}$ .

Fig. 9 presents the  $\hat{\nu}$  and  $\hat{k}$  components of the averaged tidal torque for the viscous elasticity model. The components are called  $T_\nu$  and  $T_k$ , respectively; the first causes change in  $\theta$ , and the second causes change in the spin rate  $\dot{\gamma}$ . We do not show the  $\hat{\mu}$  component of the tidal torque, because it is much smaller than the corresponding component of the permanent asymmetry torque. The  $\hat{\mu}$  component causes change in  $\psi$ ; since the asymmetry torque  $\hat{\mu}$  component dominates its differential equation, the result is a steady increase in  $\psi$ , i.e., a steady precession of the spin axis around the orbit normal axis. Although the rate of precession varies somewhat with the inclination angle

and spin rate, it is of minor importance to the spin-orbit resonance. We shall not discuss it further.

The component  $T_k$  (Fig. 9b) crosses through zero at the spin rate  $\dot{\gamma} = 1.00n$  for  $\theta = 0^\circ$ , and at  $1.29n$  for the other values of  $\theta$ . This is the spin rate below which the tidal torque cannot drive  $\dot{\gamma}$ . If the asymmetry torque did not capture the spin rate into a resonance, the spin rate would settle at the rate where the averaged k component of tidal torque is zero.  $T_k$  is large for large spin rate; since it is also negative, we should expect a very rapid decrease in spin rate with time using the viscous model. This is equivalent to the equation for  $\dot{\gamma}$  on p.45.

The component  $T_\nu$  also crosses the zero axis (Fig. 9a). This will cause a change in the sign of  $\dot{\theta}$ . For example, a inclination of  $30^\circ$  will increase if the spin rate is more than  $2.9n$ , and decrease if the spin rate is less than  $2.9n$ . This is in accord with the qualitative estimate of the differential equation for  $\dot{\theta}$  on p.45. Further, since the asymmetry torque is an odd function of the inclination (i.e., it changes sign with  $\theta$ ; see p.33),  $\theta = 0^\circ$  is an equilibrium point.

Fig. 10 displays the  $T_\nu$  and  $T_k$  components for the averaged tidal torque, step model. The  $T_k$  component crosses the axis at a spin rate of  $1.0n$  for all inclinations and tends to a maximal negative value for large spin rates. This is clear from the equation for averaged tidal torque on p.34; essentially,  $T_k$  is a sum of terms each of which is proportional to  $\sin \epsilon_{\ell m p q}$ , i.e., to  $\epsilon_{\ell m p q}$ . But these phase shifts are all of equal magnitude



in the step model, and the coefficients of the series,  $G_{2pq}(e)$ , decrease rapidly with increasing spin rate, i.e., increasing  $q$ . Thus, the sum of terms comprising  $T_k$  at large spin rates tends to a maximal negative value. As a result, the spin rate will decrease only slowly when it is large, but rapidly when it is small, as  $T_k$  is still substantially negative there.

In Fig. 11, spin rate is integrated numerically through time from various initial conditions. It is plotted against time (the dots are regularly spaced through time) and against the inclination angle, which was also numerically integrated. The equations on p. 34 were used. As predicted for the viscous model, spin rate decreases rapidly, exponentially in fact. However, the spin rate decreases only slowly when it is small (less than about  $3n$ ). Passage through resonance has been ignored in drawing these curves, for if capture does not occur, the asymmetry torque will cause no other secular change in either spin rate or inclination.

Fig. 12 shows the numerical integration of spin rate and inclination versus time for the step model. Again, predictions are borne out, for the spin rate drops slowly when it is large and rapidly when it is small.

For both elasticity models and for a wide range of initial conditions (of which those plotted are typical), it is seen that the inclination angle increases to a maximum of about  $40^\circ$  to  $70^\circ$  when the spin rate decreases to about  $3n$ .

## Resonance Capture Probabilities

Fig. 13 presents the capture probabilities at the four lowest resonances above equilibrium. The viscous model is used; the asymmetry parameter  $\beta = 10^{-4}$ . All the probabilities are low, none greater than 0.12. However, on p. 42, the probability of capture for the viscous model is seen to depend on the square root of  $\beta$ . Hence, the more asymmetric Mercury is, the higher the probabilities of capture. At these low-numbered resonances, the stroboscopic spin rate  $\dot{\psi}$  is much larger than the precession rate  $\dot{\varphi}$ , so that passage through the resonance zone takes place at a fixed value of  $\varphi$ .  $\varphi = 90^\circ$  probabilities (spin axis is perpendicular to the Sun-perihelion vector) are higher than  $\varphi = 0^\circ$  probabilities (spin axis has a component pointing to perihelion), but never by more than 0.30. Also, the effect of increasing inclination on probability is always to decrease it.

From the formula  $P = 2S/T_r$  on p. 43, we readily may understand the reason for the small probability values. The component  $T_k$  that affects spin rate changes continuously with spin rate through the resonance. Therefore, we should expect the numerator  $S$  of the probability fraction above to be quite small. In fact, it is nonzero only because the stroboscopic spin rate  $\dot{\psi}$  is not zero during resonance passage. Further, from the simple, qualitative equation for  $\ddot{\psi}$  on p. 45, we see that the tidal torque component  $T_k$  decreases with increasing inclination  $\theta$ , and hence so does the capture probability.

The picture presented by Fig. 14, the step model probabilities, is quite different. The probabilities are much larger, though they are also independent of  $\beta$ .  $\varphi = 90^\circ$  can increase the probability of capture by as much as 0.60 over the  $\varphi = 0^\circ$  probabilities. Finally, with only one exception, increased inclination decreases probabilities in odd-numbered (half-integer) resonances, but increases them in even-numbered resonances; the probabilities increase to a maximum for the inclination near  $60^\circ$ .

Again, the formula  $P = 2S/T_r$  makes this clear. For, the step model torque changes discontinuously when the spin rate passes through a resonance value. Hence the numerator  $S$  will be large, especially at low-numbered resonances, where the coefficients  $G_{2pq}$  of the torque terms are large. To determine the effect of inclination upon capture probability, we must look for the dominant term among the several that change sign at the resonance value. Clearly, it is the term with the largest  $e^{|q|}$ , where  $e$  is the eccentricity of Mercury's orbit. From (C.15), this is the term with  $G_{2pq}(e)$  for the smallest  $q$ . Since, for small inclination  $\theta$  (less than about  $60^\circ$ ), the inclination polynomials  $F_{2mp}(\theta)$  are of the order of  $\theta^{|2-2p-m|}$  (Table B.1). Finally, the time averaging has elided all terms except those for which  $(4p-4-2q)/m$  is an integer, the number of the resonance. The conclusion is that for odd-numbered resonances, the term  $F_{220}G_{20q}$  dominates; this term decreases with inclination. For even-numbered resonances,  $F_{210}G_{20q}$  dominates; this term increases with inclination, reaching a maximum at about  $60^\circ$ .

This phenomenon raises the interesting question of why Mercury's spin rate was not trapped at  $3n$  or  $2n$ , since Fig. 12 shows that an inclination of  $50^\circ$  or so is not unlikely at these spin rates. Fig. 14 shows a cumulative probability of perhaps 0.70 into a spin rate higher than the  $\frac{3}{2}n$  spin rate. Since this did not occur, this is an argument against the likelihood of the step elasticity model.

Finally, we note the anomalous increase of probability with inclination for  $\psi = 90^\circ$  at spin rate  $1.5n$ . However, the probabilities of capture are so large at  $1.5n$  that capture here is virtually certain anyway.

## BIBLIOGRAPHY

- Allen, C. W.: 1964, Astrophysical Quantities, Univ. of London, 143.
- Brouwer, D. and Van Woerkom, A. J. J.: 1950, Astron. Papers  
Amer. Ephemeris 13(Pt. 2).
- Colombo, G. and Shapiro, I. I.: 1966, Ap. J. 145, 296.
- Counselman, C. C., III: 1969, "Spin-Orbit Resonance of Mercury",  
MIT Experimental Astronomy Laboratory.
- Danby, J. M. A.: 1962, Fundamentals of Celestial Mechanics,  
MacMillan.
- Goldreich, P.: 1966, Rev. of Geoph. 4, 411.
- Goldreich, P. and Peale, S. J.: 1966, Ast. J. 71, 425.
- Goldreich, P. and Soter, S.: 1965, Icarus 5, 375.
- Jackson, J. D.: 1962, Classical Electrodynamics, Wiley, 1962.
- Kaula, W. M.: 1964, Rev. of Geoph. 2, 661.
- Knopoff, L. and MacDonald, G. J. F.: 1960, J. of Geoph. Res.  
65, 2191.
- Lomnitz, C.: 1957, J. of App. Phys. 28, 201.
- Peale, S. J.: 1974, "Possible histories of the obliquity of  
Mercury," Ast. J. 79, 722-744.
- Pettengill, G. H. and Dyce, R. B.: 1965, Nature 206, 1240.
- Wildt, R.: 1961, Planets and Satellites, eds. G. P. Kuiper and  
B. M. Middlehurst, Univ. of Chicago, 159-212.

- Brumberg, V.A.: 1967, "Development of the Perturbative Function in Satellite Problems," Akad. Nauk - Byull. Inst. Teor. Astr. XI #2, 73-84 (in Russian).
- Challe, A. & Laclaverie, J.J.: 1969, "Disturbing Function and Analytic Solution to the Problem of the Motion of a Satellite," Astron. & Astroph. 3, 15-28 (in French).
- Edmonds, A.R.: 1957, Angular Momentum in Quantum Mechanics, Princeton, 60-63.
- Erdélyi, A., Magnus, W., Oberhettinger, F. & Tricomi, F.: 1953, Higher Transcendental Functions: the Bateman Manuscript Project, McGraw-Hill, vol. I, 5, 105; vol. II, 168-174, 244, 256-259.
- Goldstein, H.: 1950, Classical Mechanics, Addison-Wesley, 116.
- Gooding, R.H.: 1971, "A Recurrence Relation for Inclination Functions," Cel. Mech. 4, 91-98.
- Jeffreys, B.S.: 1965, "Transformation of Tesseral Harmonics under Rotation," Geophys. J. 10, 141-145.
- Kaula, W.M.: 1961, "Analysis of Gravitational and Geometric Aspects of Geodetic Utilization of Satellites," Geophys. J. 5, 104-133.
- Kaula, W.M.: 1962, "Development of the Lunar and Solar Disturbing Function for a Close Satellite," Astr. J. 67, 300-303.
- Landau, L. & Lifshitz, E.: 1958, Quantum Mechanics, Addison-Wesley, 297-299, 386.
- Morse, P. & Feshbach, H.: 1953, Methods of Theoretical Physics, McGraw-Hill, 1719-1723.

- Plummer, H.C.: 1960, An Introductory Treatise on Dynamical Astronomy, Dover, 42, 158-170.
- Satô, Y.: 1950, "Transformation of Wave-functions Related to the Transformation of Coordinate Systems, II," Bull. Earthq. Res. Inst. Tokyo 28, 175-203.
- Schwinger, J.: 1952, "On Angular Momentum," in Quantum Theory of Angular Momentum, Academic Press (1965), 235-245.
- Timoshkova, E.I.: 1973, "An Expansion of the Disturbing Function," Sov. Astron.--AJ 16, 714-718.
- Wigner, E.: 1959 (German edition, 1931), Group Theory and its Application to the Quantum Mechanics of Atomic Spectra, Academic Press, Chap. 15.

## Appendix A. The Wigner Rotation Coefficients

Define the Wigner rotation coefficient functions by  
(Wigner, 1959)

$$D_{\mu\nu}^{\lambda}(\alpha, \beta, \gamma) = e^{i\mu\alpha + i\nu\gamma} \left[ \frac{(\lambda - \mu)! (\lambda - \nu)!}{(\lambda + \mu)! (\lambda + \nu)!} \right]^{1/2} P_{\lambda}^{\mu\nu}(\beta), \quad (A1)$$

where we define the reduced Wigner function by an infinite series

$$P_{\lambda}^{\mu\nu}(\beta) = \{\sin(\beta/2)\}^{\nu - \mu} \{\cos(\beta/2)\}^{\nu + \mu} \times \sum_{k=0}^{\infty} \frac{(\lambda + \nu + k)! \{-\sin^2(\beta/2)\}^k}{(\lambda - \nu - k)! (k + \nu - \mu)! k!}. \quad (A2)$$

For our purposes of definition, we shall define the angle triplet  $(\alpha\beta\gamma)$  to be the three Euler angles that rotate a right-handed coordinate system into another right-handed coordinate system. The Euler angle convention will be that used in celestial mechanics; although Wigner used a left-handed coordinate system and the quantum mechanical convention for Euler angles, we have converted his function to be consistent with our convention. Specifically, rotate by  $\alpha$  around the z axis, by  $\beta$  around the new x axis, and by  $\gamma$  around the new z axis. When this rotation is followed by a second Euler rotation  $(\delta\epsilon\zeta)$ , the composition of two rotations is equivalent to a single rotation, defined as  $(\eta\theta\iota)$ . The Wigner functions faithfully reflect this composition property; as will be proved below:

$$D_{\mu\nu}^{\lambda}(\eta, \theta, \iota) = \sum_{\kappa=-\lambda}^{\infty} D_{\mu\kappa}^{\lambda}(\alpha, \beta, \gamma) D_{\kappa\nu}^{\lambda}(\delta, \epsilon, \zeta). \quad (A3)$$



The Wigner functions are said to form a "representation of the rotation group".

1. Definition (A2) for  $P_{\lambda}^{\mu\nu}(\beta)$  is non-infinite for  $\lambda+\nu \geq 0$ ; we shall assume that this and  $\lambda+\mu \geq 0$  are true. Here is a short table. The abbreviations  $c = \cos(\beta/2)$  and  $s = \sin(\beta/2)$  are used.

$$P_0^{00} = 1;$$

$$P_{1/2}^{1/2,1/2} = c, P_{1/2}^{-1/2,1/2} = s;$$

$$P_1^{00} = \cos\beta, P_1^{01} = \sin\beta, P_1^{11} = 1+\cos\beta;$$

$$P_{3/2}^{1/2,1/2} = 6c^3-4c, P_{3/2}^{1/2,3/2} = 6sc^2, P_{3/2}^{3/2,3/2} = 6c^3;$$

$$P_2^{00} = (3\cos^2\beta-1)/2, P_2^{01} = 3\sin\beta\cos\beta, P_2^{02} = 3\sin^2\beta,$$

$$P_2^{11} = 3(2\cos^2\beta+\cos\beta-1), P_2^{12} = 6\sin\beta(1+\cos\beta), P_2^{22} = 6(1+\cos\beta)^2.$$

2. Rewriting (A2) in terms of the hypergeometric function,

$$P_{\lambda}^{\mu\nu}(\beta) = s^{\nu-\mu} c^{\nu+\mu} \frac{(\lambda+\nu)!}{(\lambda-\nu)!(\nu-\mu)!} F(\nu-\lambda, \nu+\lambda+1, \nu-\mu+1, s^2). \quad (A4a)$$

This hypergeometric series by itself is called a Jacobi polynomial in  $\cos\beta$  (Erdélyi et al., 1953). As it is one of the classical orthogonal polynomials, it possesses the usual second order differential equation, three term recursion relations, etc., all of which the Wigner functions inherit.

3. From (A2) we have immediately  $P_{\lambda}^{\mu\nu}(0) = \delta_{\mu\nu} (\lambda+\nu)!/(\lambda-\nu)!$ , (A4b)

$$P_{\lambda}^{\mu\nu}(-\beta) = (-1)^{\nu-\mu} P_{\lambda}^{\mu\nu}(\beta), \quad (A4c)$$

$$P_{\lambda}^{\mu\nu}(2\pi+\beta) = (-1)^{2\nu} P_{\lambda}^{\mu\nu}(\beta). \quad (A4d)$$

For  $2\nu$  an integer,

$$(\lambda+\nu+k)!/(\lambda-\nu-k)! = (\lambda+\nu+k)(\lambda+\nu+k-1)\dots(\lambda-\nu-k+1)$$

and changes by  $(-1)^{2\nu}$  when  $\lambda \rightarrow -\lambda-1$ ; we have from (A2)

$$P_{-\lambda-1}^{\mu\nu}(\beta) = (-1)^{2\nu} P_{\lambda}^{\mu\nu}(\beta). \quad (A4e)$$

When  $\mu - \nu$  is an integer, we may set  $k \rightarrow k + \mu - \nu$  in (A2) and get

$$P_{\lambda}^{\mu\nu}(\beta) = (-1)^{\mu-\nu} P_{\lambda}^{\nu\mu}(\beta). \quad (\text{A5})$$

Otherwise, the two functions are linearly independent, from the theory of the hypergeometric function. See also (A9). However,

$$F(a, b, c, z) = (1-z)^{c-a-b} F(c-a, c-b, c, z)$$

(Erdélyi, 1953), so for all  $\lambda, \mu, \nu$ , from (A1) and (A1),

$$D_{\mu\nu}^{\lambda}(0, \beta, 0) = D_{-\nu, -\mu}^{\lambda}(0, \beta, 0). \quad (\text{A6})$$

4. From (A2) we have immediately, for  $j$  an integer,

$$[d/d(s^2)]^j [s^{\pm(\mu-\nu)} c^{-\mu-\nu} P_{\lambda}^{\mu\nu}(\beta)] = s^{-j \pm (\mu-\nu)} c^{-j-\mu-\nu} \begin{Bmatrix} (-1)^j P_{\lambda}^{\mu, \nu+j}(\beta) \\ P_{\lambda}^{\mu+j, \nu}(\beta) \end{Bmatrix} \quad (\text{A7})$$

5. For  $t$  a dummy parameter, we may sum over (A2); interchanging  $\ell$  and  $k$  summations and using the binomial theorem:

$$\sum_{\ell=0}^{\infty} t^{\ell} P_{\ell+\nu}^{0\nu}(\beta) = (sc)^{\nu} \sum_{k=0}^{\infty} \frac{(2k+2\nu)!}{(k+\nu)!k!} (-s^2 t)^k (1-t)^{-2\nu-2k-1}$$

Use the duplication formula  $(2z)! = 2^{2z} z!(z-1/2)!/(-1/2)!$  (Erdélyi, 1953) and sum again binomially

$$= (2\sin\beta)^{\nu} [(\nu-1/2)!/(-1/2)!] [1+t^2-2t\cos\beta]^{-\nu-1/2}.$$

By (A25) then, this is a Gegenbauer function:

$$P_{\ell+\nu}^{0\nu}(\beta) = (2\sin\beta)^{\nu} [(\nu-1/2)!/(-1/2)!] C_{\ell}^{(\nu+1/2)}(\cos\beta). \quad (\text{A8})$$

Combining (A8), (A25), (A26), (A6) and (A7), we have

$$D_{0, \pm 1/2}^{\ell-1/2}(0, \beta, 0) = D_{\mp 1/2, 0}^{\ell-1/2}(0, \beta, 0) = [2/(\pi\ell\sin\beta)]^{1/2} \begin{Bmatrix} \sin\ell\beta \\ \cos\ell\beta \end{Bmatrix}. \quad (\text{A9})$$

6. Further properties are more easily obtained from a generating function. From now on, we assume that  $\lambda + \mu$  is a nonnegative integer. Summing (A2) binomially with dummy parameter  $u$  ( $< \min(|s/c|, |c/s|)$  for convergence),

$$\sum_{\mu=-\lambda}^{\infty} P_{\lambda}^{\mu\nu}(\beta) u^{\lambda+\mu} / (\lambda+\mu)! = (s+cu)^{\lambda+\nu} (c-su)^{\lambda-\nu} / (\lambda-\nu)! \quad (A10)$$

7. Set  $\nu \rightarrow -\nu$  and  $\beta \rightarrow \pi+\beta$  in (A10); we have (cf. (A9) for general  $\lambda, \mu$ )

$$P_{\lambda}^{\mu, -\nu}(\pi+\beta) = (-1)^{\lambda+\nu} [(\lambda-\nu)! / (\lambda+\nu)!] P_{\lambda}^{\mu\nu}(\beta). \quad (A11)$$

Hence 
$$P_{\lambda}^{\mu 0}(\pi+\beta) = (-1)^{\lambda} P_{\lambda}^{\mu 0}(\beta).$$

8. Set  $\nu=0$  and  $\beta=\pi/2$  in (A10); expanding by the binomial theorem,

$$P_{\lambda}^{\mu 0}(\pi/2) = \begin{cases} (-1)^k 2^{-\lambda} (2k)! / [k! (\lambda-k)!], & \text{if } \lambda+\mu=2k, \text{ an even integer;} \\ 0, & \text{otherwise.} \end{cases} \quad (A12)$$

More generally,  $P_{\lambda}^{\mu\nu}(\pi/2)$  is called a Cauchy number (Plummer, 1960).

9. Rewriting (A10),

$$\sum_{\mu=-\lambda}^{\infty} P_{\lambda}^{\mu\nu}(\beta) u^{\lambda+\mu} / (\lambda+\mu)! = (2s)^{-\lambda-\nu} (2c)^{\nu-\lambda} (1-\cos\beta + u\sin\beta)^{\lambda+\nu} (1+\cos\beta - u\sin\beta)^{\lambda-\nu} / (\lambda-\nu)!$$

This is of the form  $f(x-h)$  for  $x = \cos\beta$  and  $h = u\sin\beta$ . Expanding by Taylor's theorem and equating coefficients of  $u^{\lambda+\mu}$ , we have a

Rodrigues' formula:

$$P_{\lambda}^{\mu\nu}(\beta) = (-1)^{\lambda+\mu} 2^{-\lambda} (\sin\beta)^{\mu+\nu} (1-\cos\beta)^{-\nu} (d/d\cos\beta)^{\lambda+\mu} [(1-\cos\beta)^{\lambda+\nu} (1+\cos\beta)^{\lambda-\nu}] / (\lambda-\nu)! \quad (A13)$$

For  $\nu=0$ , this is the associated Legendre function (Erdélyi, 1953)

$$P_{\lambda}^{\mu 0}(\beta) = P_{\lambda}^{\mu}(\cos\beta) \quad (A14)$$

and the spherical harmonic

$$D_{\mu 0}^{\lambda}(\alpha, \beta, \gamma) = [4\pi / (2\lambda+1)]^{1/2} Y_{\lambda\mu}(\beta, \alpha). \quad (A15)$$

Inserting (A13) and integrating by parts repeatedly, we have

the orthogonality relation (\* means complex conjugate)

$$\int_0^{2\pi} d\alpha \int_{-1}^{+1} d\cos\beta \int_0^{2\pi} d\gamma D_{\mu\nu}^{\lambda}(\alpha\beta\gamma) D_{\mu'\nu'}^{\lambda*}(\alpha\beta\gamma) = [8\pi^2 / (2\lambda+1)] \delta_{\lambda\lambda} \delta_{\mu\mu'} \delta_{\nu\nu'} \quad (A15a)$$

10. To prove the fundamental property (A3) we introduce the Cayley-Klein matrix (Goldstein, 1950)

$$\underline{Q}(\alpha\beta\gamma) = \begin{pmatrix} \cos(\beta/2)\exp[i(\alpha+\gamma)/2] & i\sin(\beta/2)\exp[i(\gamma-\alpha)/2] \\ i\sin(\beta/2)\exp[i(\alpha-\gamma)/2] & \cos(\beta/2)\exp[i(-\alpha-\gamma)/2] \end{pmatrix}.$$

Then for the Euler rotation  $xyz \rightarrow x'y'z'$ , the transformation of coordinates is specified by

$$\begin{pmatrix} z' & x'-iy' \\ x'+iy' & -z' \end{pmatrix} = \underline{Q} \begin{pmatrix} z & x-iy \\ x+iy & -z \end{pmatrix} \underline{Q}^\dagger,$$

where  $\underline{Q}^\dagger$  is the conjugate transpose of  $\underline{Q}$ . For the composition of rotations mentioned above (A3), therefore, the corresponding matrices obey

$$\underline{Q}(\eta\theta\iota) = \underline{Q}(\delta\epsilon\zeta)\underline{Q}(\alpha\beta\gamma). \quad (\text{A16})$$

From (A10), letting  $u = e^{i\eta}$ ,  $C = \cos(\theta/2)$ ,  $S = \sin(\theta/2)$ ,

$$\sum_{\mu=-\lambda}^{\infty} P_{\lambda}^{\mu\nu}(\theta) e^{i\mu\eta+i\nu\iota}/(\lambda+\mu)! = \frac{[Se^{i(1-\eta)/2} + Ce^{i(\eta+1)/2}]^{\lambda+\nu}}{[Ce^{i(-\eta-1)/2} - Se^{i(\eta-1)/2}]^{\lambda-\nu}/(\lambda-\nu)!}$$

Substitute for  $(\eta\theta\iota)$  from (A16). Use the abbreviations  $u = e^{i\alpha}$ ,  $v = e^{i\gamma}$ ,  $c = \cos(\beta/2)$ ,  $s = \sin(\beta/2)$ ,  $u' = e^{i\delta}$ ,  $v' = e^{i\zeta}$ ,  $c' = \cos(\epsilon/2)$  and  $s' = \sin(\epsilon/2)$ . Substituting and rearranging slightly,

$$= (uvu')^{-\lambda} v'^{\nu} (c-su)^{2\lambda} [s'+c'u'v' (s+cu)/(c-su)]^{\lambda+\nu} [c'-s'u'v'(s+cu)/(c-su)]^{\lambda-\nu}/(\lambda-\nu)!$$

which by (A10)

$$= \sum_{\kappa=-\lambda}^{\infty} \frac{(u'v)^{\kappa}}{(\lambda+\kappa)!} P_{\lambda}^{\kappa\nu}(\epsilon) u^{-\lambda} v'^{\nu} [(s+cu)^{\lambda+\kappa} (c-su)^{\lambda-\kappa}].$$

Expanding the bracketed expression by (A10)

$$= \sum_{\kappa, M=-\lambda}^{\infty} \frac{(\lambda-\kappa)!}{(\lambda+\kappa)!} (u'v)^{\kappa} v'^{\nu} P_{\lambda}^{\kappa\nu}(\epsilon) \frac{u^M}{(\lambda+M)!} P_{\lambda}^{M\kappa}(\beta).$$

In the limit of small angles,  $\eta \rightarrow \alpha$ . Hence, we may identify coefficients of corresponding powers of  $e^{i\eta}$  and  $e^{i\alpha} = u$ . We obtain (A3).

Proofs of (A3) or equivalent identities are numerous. Schwinger (1952) uses generating functions, as we do. Wigner (1959) and Herglotz (Erdélyi, 1953) use the theory of the rotation group; Jeffreys (1965) and Timoshkova (1973) abbreviate such arguments.

Satô (1950), Kaula (1961), Brumberg (1967) and Challe & Laclaverie (1969) utilize elementary algebra, but only Brumberg finds as simple a form for  $P_{\lambda}^{\mu\nu}$  as (A2). Finally, Morse & Feshbach (1953) and Landau & Lifshitz (1958) derive  $P_{\lambda}^{\mu\nu}$  as the solution to certain differential equations, but do not give (A3). Kaula's inclination polynomials, as redefined in Gooding (1971) are

$$F_{\ell mp}(\beta) = i^{2p-\ell+m} P_{\ell}^{2p-\ell, 0}(\pi/2) P_{\ell}^{m, \ell-2p}(\beta).$$

11. Let  $\underline{r} = (\sin\theta\cos\phi, \sin\theta\sin\phi, \cos\theta)$ .  $(0, -\theta, -\phi-\pi/2)$  rotates  $\underline{r}$  into the z axis. Similarly,  $(\phi'+\pi/2, \theta', 0)$  rotates the z axis into  $\underline{r}'$ . Alternately,  $\underline{r}$  can be rotated directly into  $\underline{r}'$  by some  $(\alpha\beta\gamma)$ , where  $\beta$  is the angle between  $\underline{r}$  and  $\underline{r}'$ . Let  $\mu=\nu=0$  in (A3) in this case and we have proved the well known Legendre addition theorem for spherical harmonics (Erdélyi, 1953):

$$P_{\ell}(\cos\beta) = [4\pi/(2\ell+1)] \sum_{k=-\ell}^{\ell} Y_{\ell k}^*(\theta, \phi) Y_{\ell k}(\theta', \phi').$$

Similarly, rotate coordinates  $xyz \rightarrow x'y'z'$  by  $(\alpha\beta\gamma)$ . The z axis may be rotated into a vector  $\underline{r}$  by  $(\phi+\pi/2, \theta, 0)$ ; analogously, rotate the z' axis into the same  $\underline{r}$  by some  $(\phi'+\pi/2, \theta', 0)$ . By (A3) and (A15), the transformation of a spherical harmonic as seen from a rotated coordinate system is (Wigner, 1959)

$$Y_{\lambda\mu}(\theta, \phi) = \sum_{\kappa=-\lambda}^{\lambda} i^{\kappa-\mu} D_{\mu\kappa}^{\lambda}(\alpha\beta\gamma) Y_{\lambda\kappa}(\theta', \phi'). \quad (A16a)$$

This close connection of transformation coefficients and transformable functions is the cornerstone of Wigner's elegant theory of special functions.

12. A simple convolution identity is obtained by multiplying (A10) by (A10) with  $\lambda \rightarrow L-\lambda$  and  $\nu \rightarrow N-\nu$ . The result is again of the form (A10); identifying coefficients of u:

$$\binom{L-N}{\lambda-v} P_L^{MN}(\beta) = \sum_{\mu=-\lambda}^{\lambda} \binom{L+M}{\lambda+\mu} P_{\lambda}^{\mu\nu}(\beta) P_{L-\lambda}^{M-\mu, N-\nu}(\beta).$$

More elaborate identities involve the vector coupling (Clebsch-Gordan) coefficients (Schwinger, 1952 and Edmonds, 1957).

13. Recurrence relations are most easily derived from a more compact generating function. Summing (A10) binomially with parameters  $t$  and  $v$ ,

$$\sum_{\lambda=0, 1/2, 1, 3/2, \dots}^{\infty} \sum_{\mu, \nu=-\lambda}^{\lambda} P_{\lambda}^{\mu\nu}(\beta) t^{2\lambda} u^{\lambda+\mu} v^{\lambda+\nu} / [(\lambda+\mu)!(\lambda+\nu)!] = e^w, \quad (A17)$$

where

$$w = t[c(1+uv) + s(v-u)].$$

We thus restrict  $\lambda+\mu$  and  $\lambda+\nu$  to be integers, although many of the recurrence relations will be true more generally.

By definition of  $w$ ,

$$t^{-1} (\partial/\partial v) e^w = (cu+s) e^w; \quad (A18)$$

insert (A17) into (A18), perform the differentiation, and equate coefficients of  $t, u, v$  on each side:

$$P_{\lambda+1/2}^{\mu+1/2, \nu+1/2} = c(\lambda+\mu+1) P_{\lambda}^{\mu\nu} + s P_{\lambda}^{\mu+1, \nu}. \quad (A19)$$

Interchange  $\mu$  and  $\nu$ , use (A5) and subtract from (A19):

$$c(\mu-\nu) P_{\lambda}^{\mu\nu} + s(P_{\lambda}^{\mu, \nu+1} + P_{\lambda}^{\mu+1, \nu}) = 0. \quad (A20)$$

Let  $\nu \rightarrow -\nu$ , use (A11) and eliminate common terms with (A20). The result is a recursion in  $\nu$  alone:

$$P_{\lambda}^{\mu, \nu+1} + [2(\mu-\nu \cos \beta)/\sin \beta] P_{\lambda}^{\mu\nu} + (\lambda+\nu)(\lambda-\nu+1) P_{\lambda}^{\mu, \nu-1} = 0. \quad (A21)$$

From (A2),  $P_{\lambda}^{\mu\lambda} = s^{\lambda-\mu} c^{\lambda+\mu} (2\lambda)!/(\lambda-\mu)!$  and  $P_{\lambda}^{\mu, \lambda+1} = 0$  start the recursion.

Insert (A17) into

$$t^{-2} (\partial/\partial u) [t(\partial/\partial t) - v(\partial/\partial v)] e^w = [v - s/t - s(\partial/\partial t)] e^w$$

and get

$$(\lambda - \nu + 1)P_{\lambda+1}^{\mu+1, \nu} = (\lambda + \nu + 1)P_{\lambda}^{\mu+1, \nu} - (2\lambda + 2)SP_{\lambda+1/2}^{\mu+1/2, \nu+1/2}.$$

Eliminate the common term with (A19) to get

$$(\lambda - \nu + 1)P_{\lambda+1}^{\mu+1, \nu} - [\nu + (\lambda + 1)\cos\beta]P_{\lambda}^{\mu+1, \nu} + (\lambda + 1)(\lambda + \mu + 1)\sin\beta P_{\lambda}^{\mu\nu} = 0. \quad (A22)$$

Finally, let  $\lambda \rightarrow -\lambda - 1$ , use (A4e), eliminate the  $P_{\lambda}^{\mu\nu}$  term using (A22) and set  $\mu \rightarrow \mu - 1$  to get a recursion in  $\lambda$  alone:

$$\begin{aligned} \lambda(\lambda - \mu + 1)(\lambda - \nu + 1)P_{\lambda+1}^{\mu\nu} + (2\lambda + 1)[\mu\nu - \lambda(\lambda + 1)\cos\beta]P_{\lambda}^{\mu\nu} \\ + (\lambda + 1)(\lambda + \mu)(\lambda + \nu)P_{\lambda-1}^{\mu\nu} = 0. \end{aligned} \quad (A23)$$

This is Gooding's recursion (1971, eq. 18) since his function

$$A_{\ell m}^n(\beta) = [(\ell - n)! / (\ell + n)!] c^{-m-n} s^{-|m-n|} P_{\ell}^{mn}(\beta) \begin{cases} (n-m)!, & n \geq m \\ (-1)^{n+m} (n+m)! / (2m)!, & n < m \end{cases}$$

Allan's two recursions (in Gooding's paper) are just the reduplication of (A19) and the same with  $\nu \rightarrow -\nu$ .

14. Finally, we derive a differential equation for our functions by inserting (A7) into (A21):

$$[(d^2/d\beta^2) + \cot\beta(d/d\beta) + \lambda(\lambda + 1) + (2\mu\nu\cos\beta - \mu^2 - \nu^2)/\sin^2\beta]P_{\lambda}^{\mu\nu}(\beta) = 0. \quad (A24)$$

15. For completeness, here are two useful expansions. The Gegenbauer polynomials are defined by

$$[1 + x^2 - 2x \cos\theta]^{-n/2} = \sum_{\ell=0}^{\infty} x^{\ell} C_{\ell}^{(n/2)}(\cos\theta), \quad (A25)$$

convergent for  $|x| < 1$ ; while a particular expansion for  $n=2$  is

$$[1 + x^2 - 2x \cos\theta]^{-1} = \sum_{\ell=0}^{\infty} x^{\ell} \frac{\sin(\ell+1)\theta}{\sin\theta} \quad (A26)$$

easily proved by noting that both sides are equal to

$$\text{Imag}\left\{ \frac{1}{[1 - x \exp(i\theta)]x \sin\theta} \right\}.$$

Appendix B. Spherical Harmonics  $Y_{\ell m}$  and Inclination Polynomials  $F_{\ell mp}$

The spherical harmonic  $Y_{\ell m}(\theta, \varphi)$  is defined by (A15) as

$$(B1) \quad Y_{\ell m}(\theta, \varphi) = D_{\ell m} \exp(im\varphi) P_{\ell}^{m0}(\theta)$$

where the normalization factor is

$$(B2) \quad D_{\ell m} = \sqrt{\frac{2\ell+1}{4\pi} \frac{(\ell-m)!}{(\ell+m)!}}$$

In our formulas for the torque of the Sun on Mercury, we have the spherical harmonic  $Y_{\ell m}(\Theta, \Phi)$ , where the angles are the spherical coordinates of the planet-Sun vector as seen from the  $\hat{i}\hat{j}\hat{k}$ , planet fixed coordinate system. We wish to express these spherical harmonic functions in terms of  $Y_{\ell m}(\Theta', \Phi')$ , where the angles are the spherical coordinates of the planet-Sun vector as seen from the  $\hat{x}\hat{y}\hat{z}$ , orbit fixed coordinate system. Since the planet-Sun vector lies in the  $\hat{x}\hat{y}$  plane at all times, this being the orbit plane, at an angle of  $f$  (the true anomaly) from the  $\hat{x}$  axis, it is clear that the spherical coordinates of the planet-Sun vector in the  $\hat{x}\hat{y}\hat{z}$  system are  $(\frac{\pi}{2}, f)$ .

The  $\hat{x}\hat{y}\hat{z}$  coordinate system is rotated into the  $\hat{i}\hat{j}\hat{k}$  system by the Euler angles  $(\psi, \theta, \varphi)$ ; therefore, the  $\hat{i}\hat{j}\hat{k}$  system is rotated into the  $\hat{x}\hat{y}\hat{z}$  system by the inverse rotation, Euler angles  $(-\varphi, -\theta, -\psi)$ . We now insert these angles into formula (A16a), which expresses the spherical harmonic functions at a point seen from one coordinate system in terms of the spherical harmonics as seen from another system:



$$(B3) \quad Y_{\ell m}(\Theta, \Phi) = \sum_{k=-\ell}^{\ell} i^{k-m} D_{mk}^{\ell}(-\gamma, -\theta, -\varphi) Y_{\ell k}(\frac{\pi}{2}, f)$$

Divide both sides of (B3) by the normalizing factor  $D_{\ell m}$  from (B2) and substitute the definition of the Wigner rotation coefficient  $D_{mk}^{\ell}$  from (A1) and the definition of  $Y_{\ell k}$  from (B1):

$$(B4) \quad Y_{\ell m}(\Theta, \Phi)/D_{\ell m} = \sum_k i^{k-m} \frac{(\ell-k)!}{(\ell+k)!} P_{\ell}^{mk}(-\theta) P_{\ell}^{k0}(\frac{\pi}{2}) \exp[ik(f-\varphi) - im\gamma]$$

Equation (A12) says that  $P_{\ell}^{k0}(\pi/2)$  is zero unless  $\ell+k$  is even. Define a new index of summation  $p$  by setting  $k = \ell - 2p$ . Substitute into (B4) with equations (A4b) and (A12) to simplify it. We obtain

$$(B5) \quad Y_{\ell m}(\Theta, \Phi)/D_{\ell m} = \sum_{p=0}^{\ell} i^{\ell+m} F_{\ell mp}(\theta) \exp[i(\ell-2p)(f-\varphi) - im\gamma]$$

where we have defined the inclination polynomial  $F_{\ell mp}$  by

$$(B6) \quad F_{\ell mp}(\theta) = \frac{(2p)!}{2^{\ell} p! (\ell-p)!} P_{\ell}^{m, \ell-2p}(\theta)$$

For reference, here is a table of all these functions, computed from the definitions.

$\ell$	$m$	$p$	$D_{\ell m}$	$Y_{\ell m}(\theta, \varphi)/D_{\ell m}$	$F_{\ell mp}(\theta)$
0	0	0	$\sqrt{\frac{1}{4\pi}}$	1	1
1	0	0	$\sqrt{\frac{3}{4\pi}}$	$\cos \theta$	$\frac{1}{2} \cos \theta$
1	0	1			$-\frac{1}{2} \sin \theta$
1	1	0	$\sqrt{\frac{3}{8\pi}}$	$-\sin \theta e^{i\varphi}$	$\frac{1}{2} (1 + \cos \theta)$
1	1	1			$\frac{1}{2} (1 - \cos \theta)$
2	0	0	$\sqrt{\frac{5}{4\pi}}$	$\frac{1}{2} (3 \cos^2 \theta - 1)$	$\frac{3}{8} \cos^2 \theta$
2	0	1			$\frac{1}{4} (3 \cos^2 \theta - 1)$

$l$	$m$	$p$	$D_{lm}$	$Y_{lm}(\theta, \varphi) / D_{lm}$	$F_{lmp}(\theta)$
2	0	2			$\frac{3}{8} A m^2 \theta$
2	1	0	$\sqrt{\frac{5}{24\pi}}$	$-3 a m \theta \cos \theta \exp(i\varphi)$	$\frac{3}{4} a m \theta (1 + \cos \theta)$
2	1	1			$-\frac{3}{2} a m \theta \cos \theta$
2	1	2			$\frac{3}{4} a m \theta (\cos \theta - 1)$
2	2	0	$\sqrt{\frac{5}{96\pi}}$	$3 a m^2 \theta \exp(i2\varphi)$	$\frac{3}{4} (1 + \cos \theta)^2$
2	2	1			$\frac{3}{2} a m^2 \theta$
2	2	2			$\frac{3}{4} (1 - \cos \theta)^2$

Table B1

Appendix C. Hansen Functions  $G_{lpq}^{mn}(e)$

Definition. The Hansen function  $X_k^{mn}(e)$  is defined as a Fourier coefficient:

$$(C.1) \quad \left(\frac{r}{a}\right)^m \exp(inf) = \sum_{k=-\infty}^{\infty} X_k^{mn}(e) \exp(ikM)$$

for  $r$  the radius,  $a$  the semi-major axis,  $e$  the eccentricity,  $f$  the true anomaly, and  $M$  the mean anomaly in the orbit.

Hence

$$(C.2) \quad X_k^{mn}(e) = \frac{1}{2\pi} \int_0^{2\pi} dM \left(\frac{r}{a}\right)^m \exp(inf - ikM).$$

For  $E$  the eccentric anomaly, we use identities from Danby (1962) (6.3.12, 1.3.8, 6.3.17, 6.3.18):

$$(C.3) \quad \begin{aligned} M &= E - e \sin E \\ \frac{r}{a} &= 1 - e \cos E = \left(1 - \frac{h}{z}\right)(1 - hz) / (1 + h^2) \\ \exp(if) &= [\cos E - e + i\sqrt{1-e^2} \sin E] / [1 - e \cos E] = hz \left(1 - \frac{h}{z}\right) / (1 - hz) \end{aligned}$$

where we define

$$(C.4) \quad \begin{aligned} z &= \exp(iE) \\ h &= \frac{e}{1 + \sqrt{1-e^2}} \end{aligned}$$

(If we let  $e = \sin \epsilon$ , then  $h = \tan(\epsilon/2)$ ) Substituting,

$$(C.5) \quad \begin{aligned} X_k^{mn}(e) &= \frac{1}{2\pi} \int_0^{2\pi} \left[ dE \frac{\left(1 - \frac{h}{z}\right)(1 - hz)}{1 + h^2} \right] \left[ \frac{\left(1 - \frac{h}{z}\right)^m (1 - hz)^m}{(1 + h^2)^m} \right] \\ &\quad \times \left[ \frac{z^n \left(1 - \frac{h}{z}\right)^n}{(1 - hz)^n} \right] \left[ z^{-k} \exp(ike \sin E) \right] \end{aligned}$$

If not for the very complicated branch cut at  $z = 0$  due to  $\exp(ikesinE) = \exp(ke(z-1/z)/2)$ , this would be a contour integral around  $|z| = 1$  and a closed form could be found for the Hansen function.

Instead, expand  $(1-h/z)^{1+m+n}$  and  $(1-hz)^{1+m-n}$  by the binomial theorem ( $\binom{m}{n}$  is the binomial coefficient  $m!/n!(m-n)!$ ):

$$(C.6) \quad X_k^{mn}(e) = \frac{1}{2\pi} \int_0^{2\pi} dE (1+h^2)^{-m-1} \sum_{s,t=0}^{\infty} \binom{1+m+n}{s} \binom{1+m-n}{t} (-h)^{s+t} \times \\ \times z^{t-s+n-k} \exp(ike \sin E)$$

Now, exchange summation and integration, and use  $z = \exp(iE)$  and the Bessel function

$$J_n(x) = \frac{1}{2\pi} \int_0^{2\pi} dE \exp(ix \sin E - inE)$$

giving

$$(C.7) \quad X_k^{mn}(e) = (1+h^2)^{-m-1} \sum_{s=0}^{\infty} \sum_{t=0}^{\infty} \binom{1+m+n}{s} \binom{1+m-n}{t} (-h)^{s+t} J_{s-t+k-n}(ke)$$

Now define

$$(C.8) \quad G_{\ell p q}(e) = X_{\ell-2p+q}^{-\ell-1, \ell-2p}(e)$$

$$(C.9) \quad = (1+h^2)^{\ell} \sum_{s=0}^{\infty} \sum_{t=0}^{\infty} \binom{-2p}{s} \binom{-2(\ell-p)}{t} (-h)^{s+t} J_{s-t+q}(\ell-2p+q)e$$

where as usual

$$\binom{-a}{s} = \frac{(-a)(-a-1)\dots(-a-s+1)}{s!} = (-1)^s \binom{a+s-1}{s}, \quad s \geq 0.$$

From (C.1) and (C.8) we have

$$(C.10) \quad \left(\frac{r}{a}\right)^{-\ell-1} \exp(i(\ell-2p)t) = \sum_{q=-\infty}^{\infty} G_{\ell p q}(e) \exp(i(\ell-2p+q)M)$$

Symmetry. From (C.2), since both  $f$  and  $M$  are odd around the same origin,

$$(C.11) \quad X_{-k}^{m,-n}(e) = X_k^{mn}(e) \quad \text{hence}$$

$$(C.12) \quad G_{\lambda, \lambda-p, -q}(e) = G_{\lambda p q}(e) \quad \text{and is real.}$$

Hence only  $q \geq 0$  need be considered.

Table. From (C.9),

$$(C.13) \quad \begin{aligned} G_{20q}(e) &= (1+h^2)^2 \sum_{t=0}^{\infty} \binom{t+3}{t} h^t J_{q-t}((q+2)e) \\ G_{22q}(e) &= (1+h^2)^2 \sum_{s=0}^{\infty} \binom{s+3}{s} h^s J_{q+s}((q-2)e) \\ G_{21q}(e) &= \sum_{r=-\infty}^{\infty} \left\{ \left[ \frac{1+h^2}{1-h^2} \right]^3 + |r| \left[ \frac{1+h^2}{1-h^2} \right]^2 \right\} h^{|r|} J_{q+r}(qe) \end{aligned}$$

where we have let  $r = s - t$  and performed a summation analytically. Note that

$$(C.14) \quad \begin{aligned} G_{222}(e) &= 0 \\ G_{210}(e) &= (1-e^2)^{-3/2} \end{aligned}$$

Limits. For small  $x$ ,  $J_n(x)$  is of the order of  $x^{|n|} / |n|!$ . Since  $h \cong e/2$ , the dominant term for small  $e$  is the  $h^0$  term, so for  $q \geq 0$ ,

$$(C.15) \quad G_{20q}(e) \cong G_{22q}(e) \cong G_{21q}(e) = O\left(\frac{(qe)^q}{q!}\right)$$

Appendix D. Generalized Inertia Coefficients  $I_{\ell m}$

Definition.

$$(D.1) \quad I_{\ell m}(\underline{R}) = \frac{4\pi}{2\ell+1} D_{\ell m} \int d\Omega' r'^{\ell} Y_{\ell m}^*(\theta', \varphi')$$

where the integral is taken over the planetary volume, a function of  $\underline{R}$ .

The distribution in mass due to a perturbing body such as the Sun changes with  $\underline{R}$ , the Sun's position. It is approximated by a tidal bulge lagging slightly behind (or ahead of) the subsolar point.

Assuming the Sun to be a spherical mass  $M_{\odot}$  at  $\underline{R}$ , the potential per unit mass felt at  $\underline{r}'$  inside the planet is

$$(D.2) \quad V(\underline{r}', \underline{R}) = \frac{GM_{\odot}}{|\underline{r}' - \underline{R}|} \\ = \sum_{L,M} GM_{\odot} \frac{r'^L}{R^{L+1}} \frac{4\pi}{2L+1} Y_{LM}(\theta', \varphi') Y_{LM}(\theta, \Phi)$$

For an incompressible planet, the change in surface radius is proportionate to the above potential, with the  $L$ 'th term multiplied by a dimensionless Love number  $k_L$ , divided by  $g$ , the surface gravity, and lagging in phase behind the Sun's true position (Counselman, 1967, p 67-70), i.e. let

$$r_0 = \text{unstressed surface radius} = r_0(\theta', \varphi')$$

$$(D.3) \quad \delta r_0 = \sum_{L,M} \frac{k_L}{g} GM_{\odot} r_0^L \frac{4\pi}{2L+1} Y_{LM}(\theta', \varphi') [R^{-L-1} Y_{LM}^*(\theta, \Phi)]_{\text{lagging}}$$

Letting  $d\Omega'$  be the element of solid angle and  $\rho(r')$  be the density,

$$\begin{aligned}
(D.4) \quad I_{\ell m}(\underline{R}) &= \left[ \int_0^{r_0 + \delta r_0} dr' r'^2 \rho(r') \int d\Omega' \right] \left[ r'^{\ell} Y_{\ell m}^*(\theta', \varphi') \right] \frac{4\pi D_{\ell m}}{2\ell+1} \\
&= \left[ \int_0^{r_0} dr' \rho(r') r'^2 \int d\Omega' + \int_{r'=r_0} d\Omega' r_0^2 \rho(r_0) \delta r_0 \right] \times \\
&\quad \times \left[ r'^{\ell} Y_{\ell m}^*(\theta', \varphi') \right] \frac{4\pi D_{\ell m}}{2\ell+1} \\
&\equiv I_{\ell m}^{(1)} + I_{\ell m}^{(2)}(\underline{R})
\end{aligned}$$

i.e., the integral over the whole planet splits into the integral over the unstressed planet plus a surface integral over the bulge.

For  $l = 2$  the first integral is defined in terms of the usual inertia coefficients (Danby, 1962, p 87):

$$(D.5) \quad \begin{pmatrix} A & -F & -G \\ -F & B & -H \\ -G & -H & C \end{pmatrix} = \int dm' \left[ r'^2 (\text{Identity matrix}) - \underline{r}' \underline{r}' \right]$$

taken around  $\hat{i}\hat{j}\hat{k}$ . Substituting for  $Y_{\ell m}(\theta, \varphi)$  from table (B.1), we find

$$\begin{aligned}
(D.6) \quad I_{00}^{(1)} &= \text{mass of planet} \\
I_{1m}^{(1)} &= 0 \\
I_{22}^{(1)} &= -\frac{iF}{4} + \frac{B-A}{8} \\
I_{21}^{(1)} &= \frac{iH}{2} - \frac{G}{2} \\
I_{20}^{(1)} &= \frac{A+B}{2} - C
\end{aligned}$$

If  $\hat{i}\hat{j}\hat{k}$  are the principal axes of inertia for the planet

$F = G = H = 0$ . We define

$$\begin{aligned}
(D.7) \quad \beta &= \frac{B-A}{C} \\
\gamma &= 1 - \frac{A+B}{2C} > 0
\end{aligned}$$

Then

$$(D.8) \quad \begin{aligned} I_{22}^{(1)} &= \frac{\beta C}{8} \\ I_{21}^{(1)} &= 0 \\ I_{20}^{(1)} &= -\gamma C \end{aligned}$$

For a check, substitute these  $I_{\ell m}$  into the expansion of the gravitational potential on p. 25; we obtain

$$(D.9) \quad U(\underline{r}''') = -\frac{G(\text{mass of planet})}{r'''} - \frac{G}{2r'''^3} \left\{ \frac{3}{2} \sin^2 \theta'' [ (B-A) \cos 2\psi'' + 2H \sin 2\psi'' ] + 6 \sin \theta'' \cos \theta'' (G \cos \psi'' + F \sin \psi'') + (3 \cos^2 \theta'' - 1) \left( \frac{A+B}{2} - C \right) \right\} + O(r'''^{-4})$$

Cf. MacCullagh's formula (Danby, 1962, p 98):

$$(D.10) \quad U(\underline{r}''') = -\frac{G(\text{mass of planet})}{r'''} - \frac{G}{2r'''^3} [A+B+C-3I] + O\left(\frac{1}{r'''^4}\right)$$

where  $I$  is the moment of inertia around  $\underline{r}''$ .

The bulge integrals

$$(D.11) \quad I_{\ell m}^{(2)}(\underline{R}) = \frac{4\pi D_{\ell m}}{2\ell+1} \int d\Omega' r_0^2 \rho(r_0) \sum_{L,M} \frac{k_L}{g} G M_0 r_0 \frac{4\pi}{2L+1} \times \\ \times Y_{LM}(\theta', \varphi') r_0^L Y_{\ell m}^*(\theta', \varphi') \left[ R^{-L-1} Y_{LM}^*(\Theta, \Phi) \right]_{\text{logging}}$$

By orthonormality (A15) and (A15a)

$$\int d\Omega' Y_{LM}(\theta', \varphi') Y_{\ell m}^*(\theta', \varphi') = \delta_{L\ell} \delta_{Mm};$$

using the expansions into Fourier series from p.31,



$$\begin{aligned}
 \text{(D.12)} \quad I_{lm}^{(z)}(\underline{R}) &= r_0^{2l+2} \rho(r_0) \left( \frac{4\pi}{2l+1} \right)^2 D_{lm} \frac{k_2}{g} GM_0 [R^{-l-1} Y_{lm}^*(\Theta, \Phi)] \text{lagging} \\
 &= r_0^{2l+2} \rho(r_0) \left[ \frac{4\pi D_{lm}}{2l+1} \right]^2 \frac{k_2}{g} GM_0 a^{-l-1} \sum_{PQ} \exp(-i\nu_{lmPQ} - i\epsilon_{lmPQ}) \\
 &\quad \times r^{-l-m} F_{lmP}(\theta) G_{lPQ}(e).
 \end{aligned}$$

where  $\epsilon_{lmPQ}$  is the phase lag.

Symmetry. From (D.1),

$$\begin{aligned}
 \text{(D.13)} \quad I_{l,-m} &= \frac{4\pi D_{l,-m}}{2l+1} \int d\Omega' r'^l Y_{l,-m}^*(\theta', \psi') \\
 &= \frac{(l+m)!}{(l-m)!} (-i)^m I_{lm}^*
 \end{aligned}$$

Inserting this into (D.12), we see

$$\text{(D.14)} \quad \epsilon_{l,-m, l-p, -q} = -\epsilon_{lmPQ}$$

which is the same symmetry as  $\nu_{lmpq}$ .

## Appendix E. Comparison with Peale's paper

Peale (1974) investigates a similar problem to that in this thesis. He uses the same technique (expansion into Fourier series), and finds similar results (capture probabilities and evolution of obliquity). The major differences are that he neglects to compute capture probabilities for other than the 3:2 resonance (which I found to be anomalous) and devotes much space to Cassini state evolution and stability. Since Mercury is apparently in a Cassini stable state with obliquity near  $0^\circ$  (an assumption made in this thesis anyway) this Cassini analysis is interesting but not necessarily applicable to Mercury.

### Peale's Approach via Hamiltonian Formulation

Peale assumes principal axis rotation, as I do, so that the only variables of interest are the three defining the spin axis. He then writes down the Hamiltonian in terms of these three angles and the differential equations for them. In order to explicitly differentiate the tidal and asymmetry potentials in the Hamiltonian, he expands them in terms of the orbit and spin axis variables ( $a, e, i$ , etc.) by the Fourier series, using Hansen coefficients and Kaula's inclination functions. These expansions are essentially identical to the ones I use. To model the tidal dissipation, he introduces a lag variable in each term of the Fourier series. Peale's two models for the phase lags (which are just the values of  $\frac{1}{Q}$ ) are  $\frac{1}{Q}$  proportional to frequency (i.e.,

MacDonald's, or viscous, model) and  $\frac{1}{Q} = \text{constant}$  (Darwin's, or step, model). Again, the technique is virtually the same as mine.

### Cassini State Analysis

Peale finds which positions of the spin axis are stable when the orbit is precessing (Cassini states) simply by finding the consequences of inserting the equations "spin rate=constant", and "spin axis position=constant" into his Hamiltonian equations. He finds easily that the longest axis of Mercury points to the Sun at perihelion, etc. Also, it is plain that the restoring torque becomes weaker as obliquity grows larger. Hence, as he found for Venus, a  $180^\circ$  obliquity is unstable in the absence of other torques. More important, large obliquities in general (about  $90^\circ$  or greater) are probably unstable. He then computes capture probability for the step model torque into the 3:2 resonance and finds a sharp decrease for obliquity larger than  $90^\circ$ . This curve agrees with my curve for that resonance (and tidal model) in both shape and amplitude. However, Peale does not, though he could have, computed capture probability for 2:1 resonance; I found that for Darwin torque, though not for MacDonald, the probability increases with obliquity in this resonance, and peaks at about  $60^\circ$ .

### Evolution of Obliquity

Peale now numerically integrates the simultaneous change of spin rate and obliquity through time. His general result is the same as mine: That obliquity increases as spin rate decreases,

until the spin rate falls below about  $3n$ . For spin rate less than this, we both find a decreasing obliquity.

Peale explores three further aspects of the model. He investigates the three Cassini states other than Mercury's current one (i.e. the states: Obliquity near  $90^\circ$ , near  $180^\circ$ , and near  $270^\circ$ ). Secondly, he averages the differential equations over a spin axis precession period (which is far less than the time of tidal decay). Thirdly, he varies the value of the flattening coefficient of Mercury's shape ( $1 - (\frac{A+B}{2C})$ ) from less than  $10^{-6}$  (i.e., hydrostatic equilibrium flattening) to  $10^{-4}$  (i.e., the Moon's flattening), since he knows from his Cassini analysis that not all four Cassini states are possible at every value of the flattening. Lastly, he briefly considers the effect of changing the orbit parameters (primarily the inclination). The major result of this portion of his paper is that the Moon and Mercury are probably in different Cassini states.

## FIGURE CAPTIONS

- Fig. 1. The three coordinate systems used in this thesis, and the Euler angle rotations connecting them.
- Fig. 2. Stroboscopic "photographs" of Mercury taken at every perihelion passage. The stroboscopic spin rate  $\dot{\psi}_0$  is positive.
- Fig. 3. Escape of Mercury from a spin-orbit resonance state, as seen stroboscopically at each perihelion passage.  $\dot{\psi}_0$  has just turned negative, as this is the last "roll forward".
- Fig. 4. Libration of Mercury in a spin-orbit resonance state.
- Fig. 5. Phase space diagram of the kinetic energy of Mercury vs. the stroboscopic spin rate, showing evolution through time.
- Fig. 6. Division of the orbit of Mercury into sectors of positive and negative torque. The arrows indicate the direction of the long end of Mercury's equatorial silhouette. Note that the long end points to the Sun at perihelion.
- Fig. 7. Same diagram as Fig. 6, except that the long end does not quite point at the Sun at perihelion.
- Fig. 8. Projection of the path of the long end on the orbital plane. (a) Zero inclination. (b) Non-zero inclination.
- Fig. 9. Averaged tidal torque components versus spin rate, viscous elasticity model. (a) Component  $T_y$ , affecting the inclination. (b) Component  $T_k$ , affecting the spin rate.  $e=.20$ ,  $\alpha/Q = .5 \times 10^{-11}$ .
- Fig. 10. Same as Fig. 9, step elasticity model.
- Fig. 11. Numerical integration of the spin rate  $\dot{\psi}$  and inclination  $\theta$  through time.  $e = .20$ ,  $\alpha = 10^{-8}$ ,  $Q = 200$ . Dots are placed on

the integration every  $10^{10}/2\pi$  orbits of Mercury, beginning at the high spin rate end. Viscous elasticity model.

Fig. 12. Same as Fig. 11, except for the step elasticity model. Dots are placed every  $5 \times 10^{10}/2\pi$  orbits.

Fig. 13. Capture probabilities into various resonance states for the viscous elasticity model.  $e, \varphi, \theta, \dot{\gamma}$  are as shown.  $\beta = 10^{-4}$ . The probabilities are proportional to the square root of  $\beta$ .

Fig. 14. Same as Fig. 13 for the step elasticity model. The probabilities are independent of  $\beta$ .

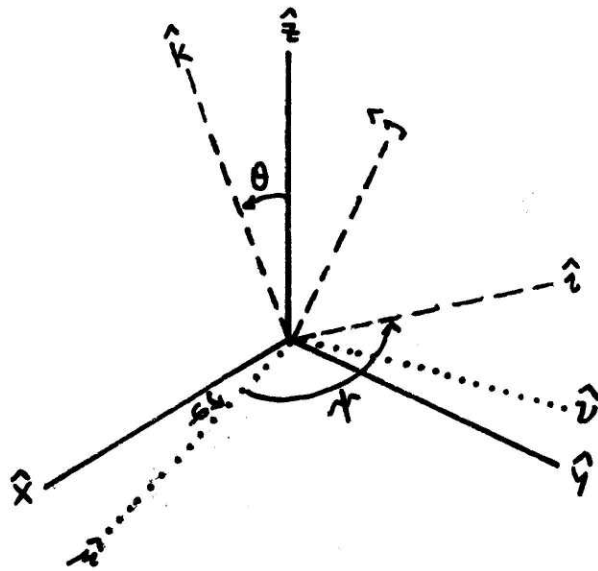
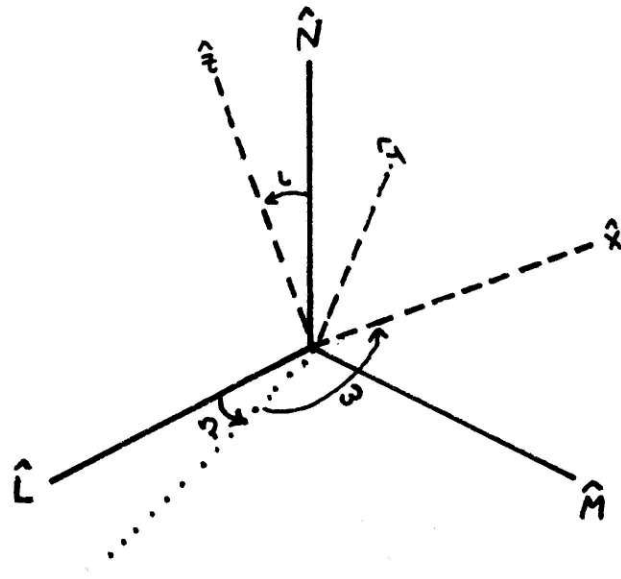


Fig. 1

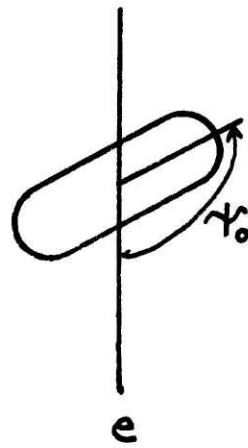
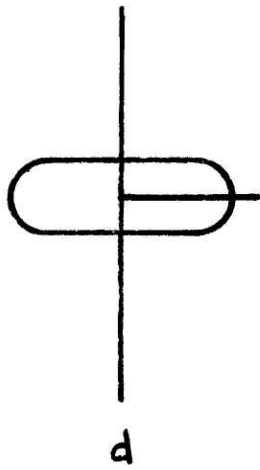
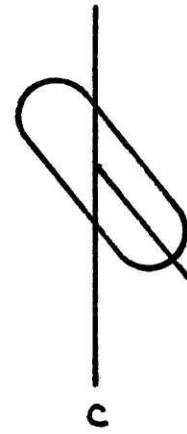
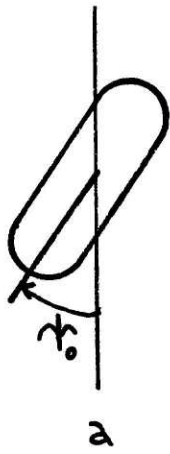


Fig. 2



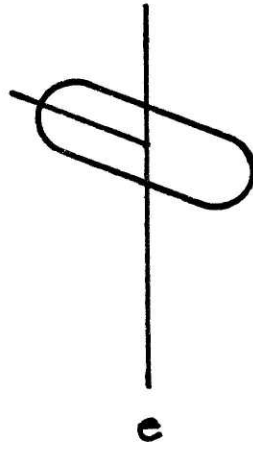
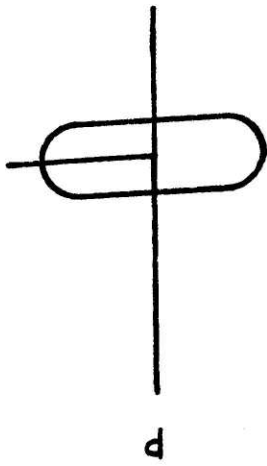
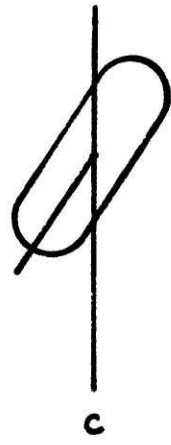
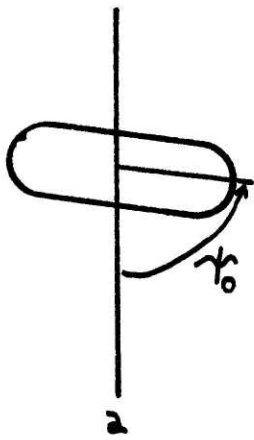


Fig. 3

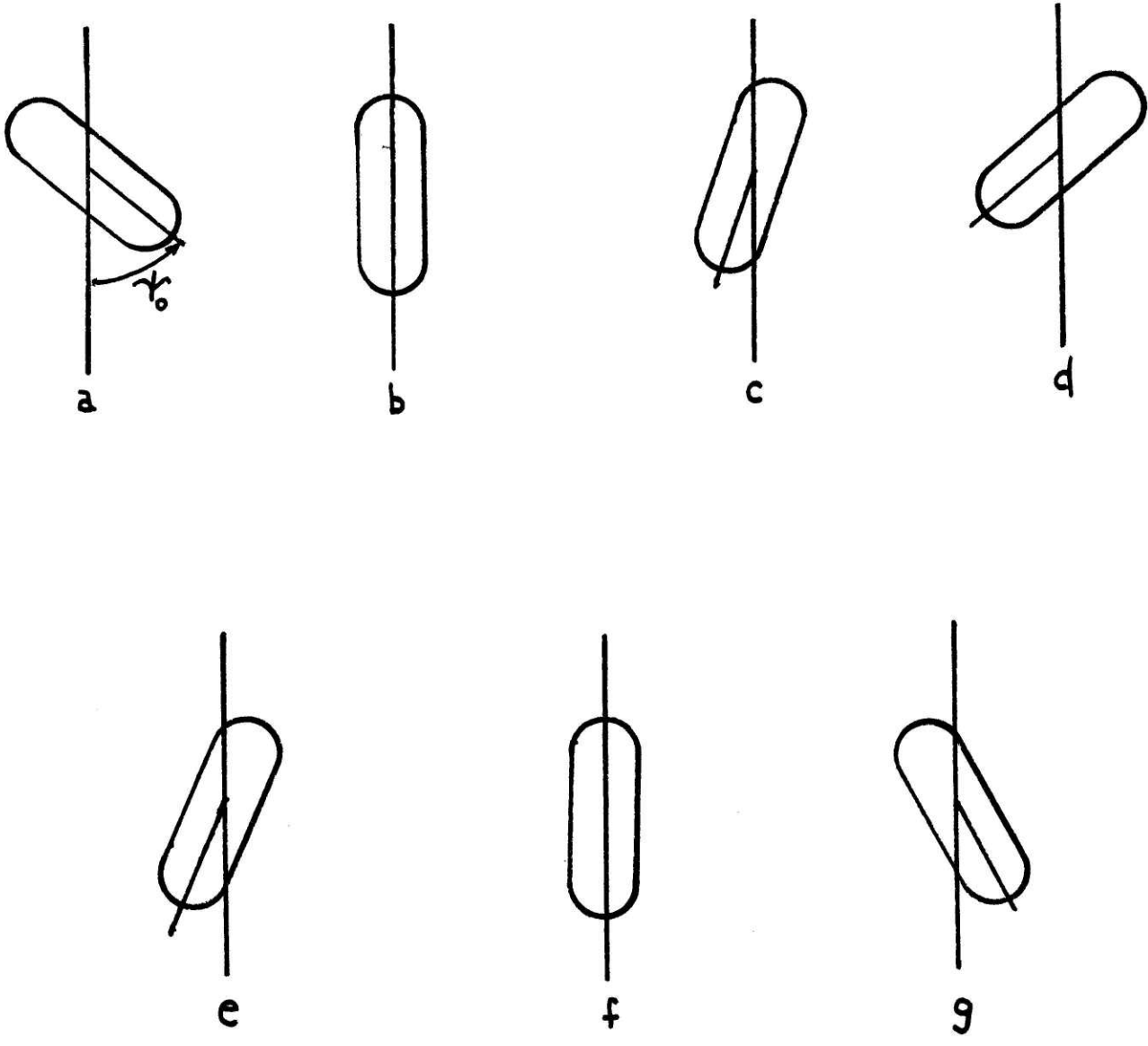


Fig. 4

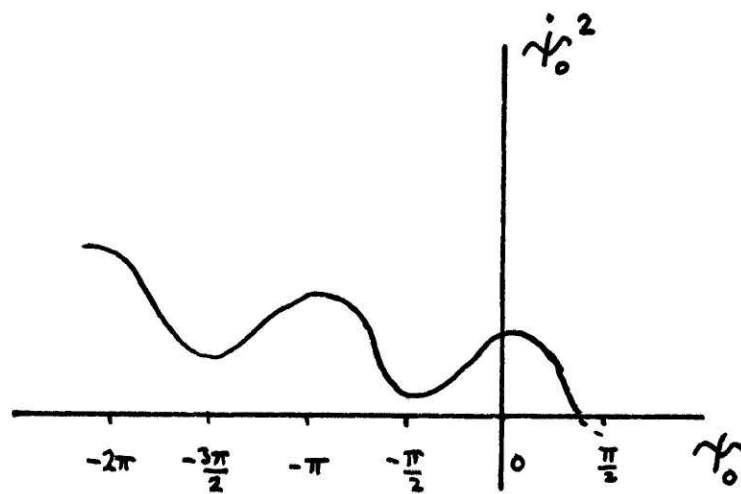


Fig. 5

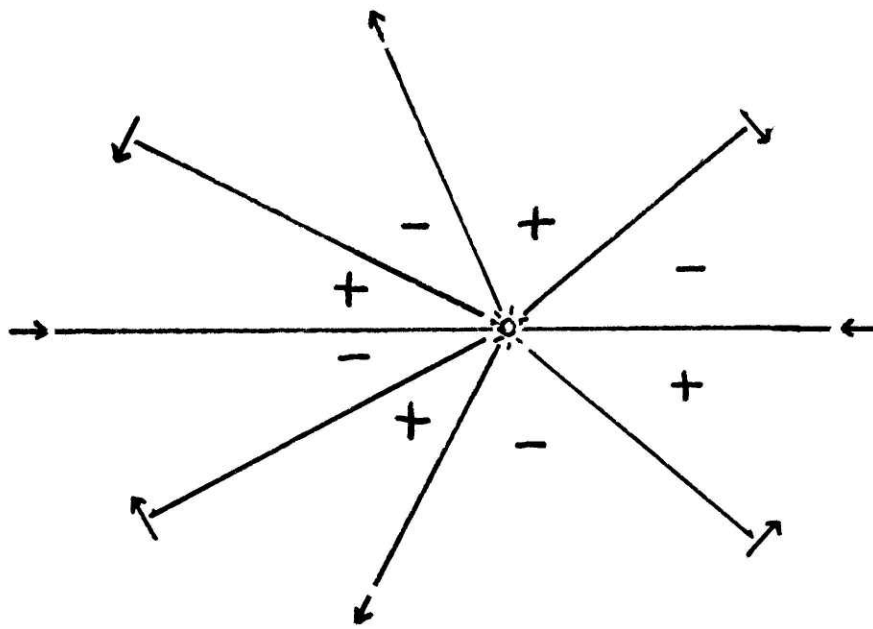


Fig. 6

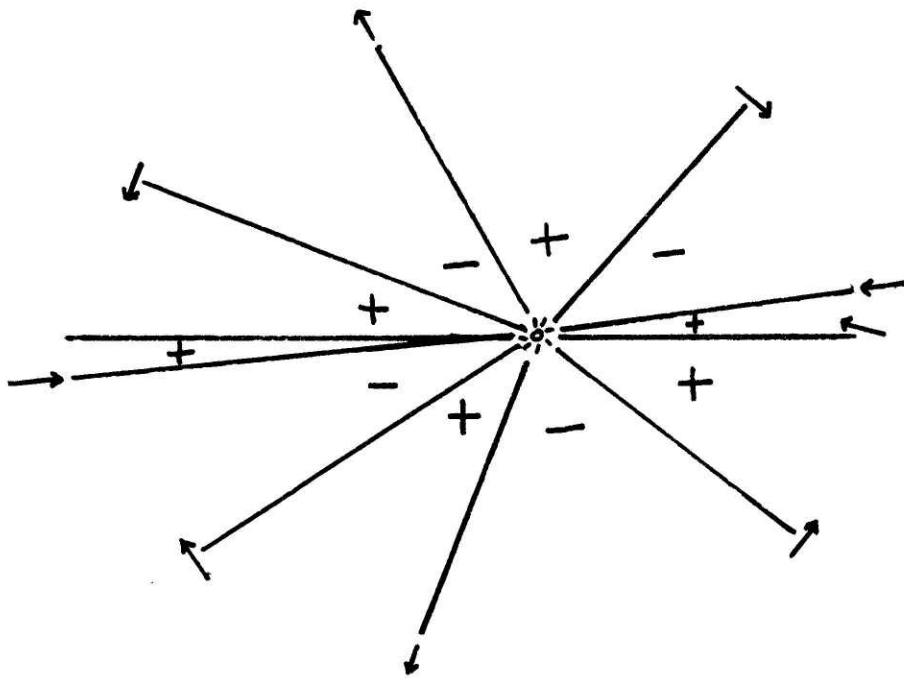
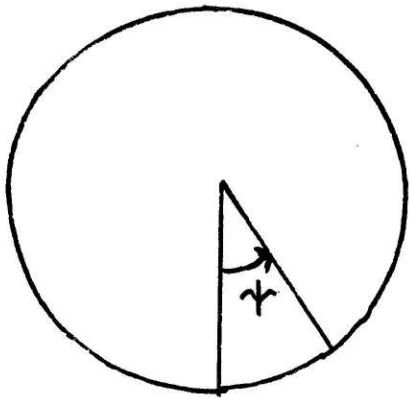
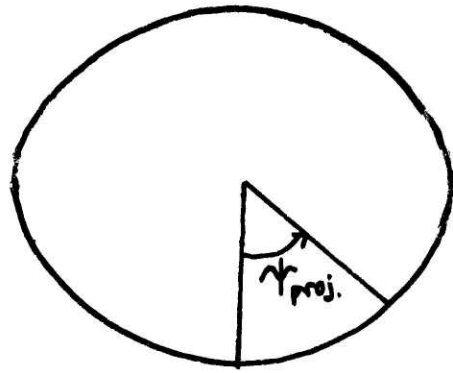


Fig. 7



a



b

Fig. 8

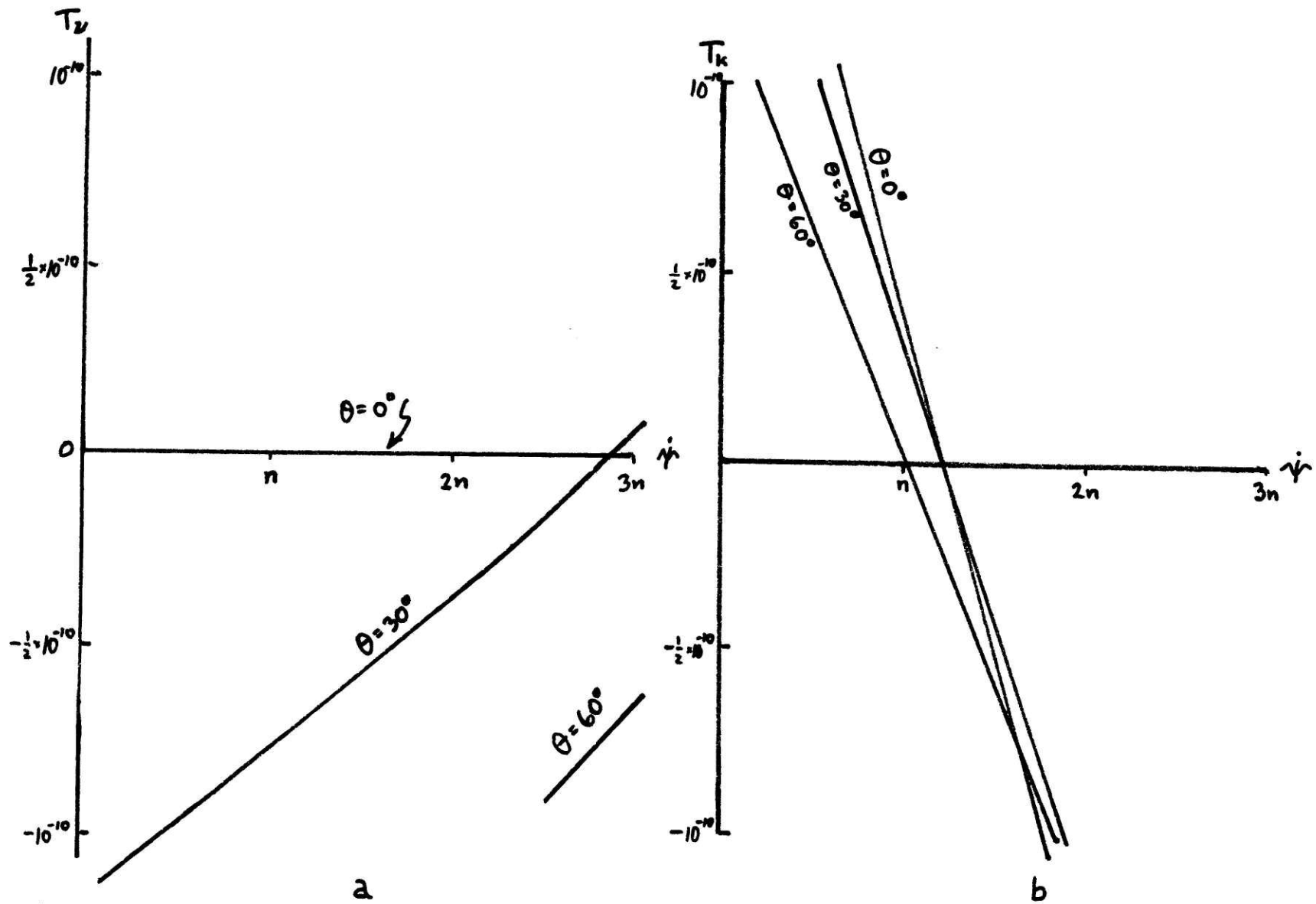
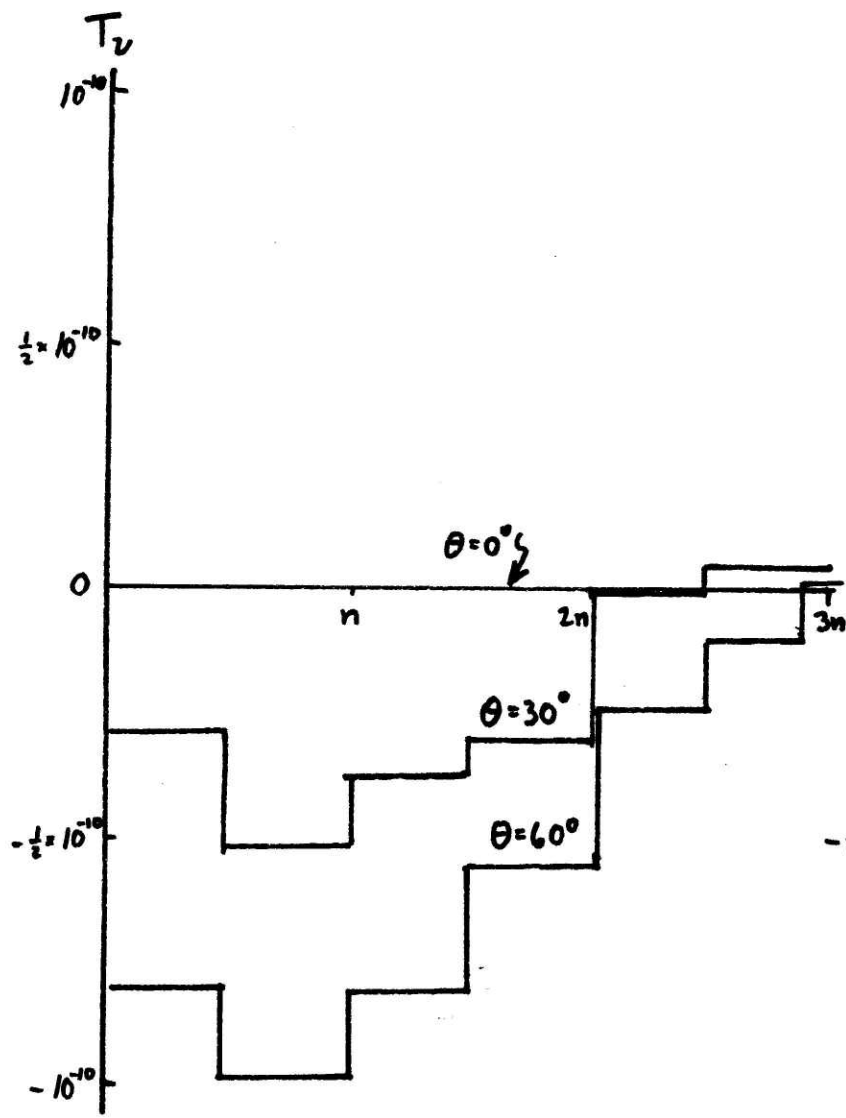
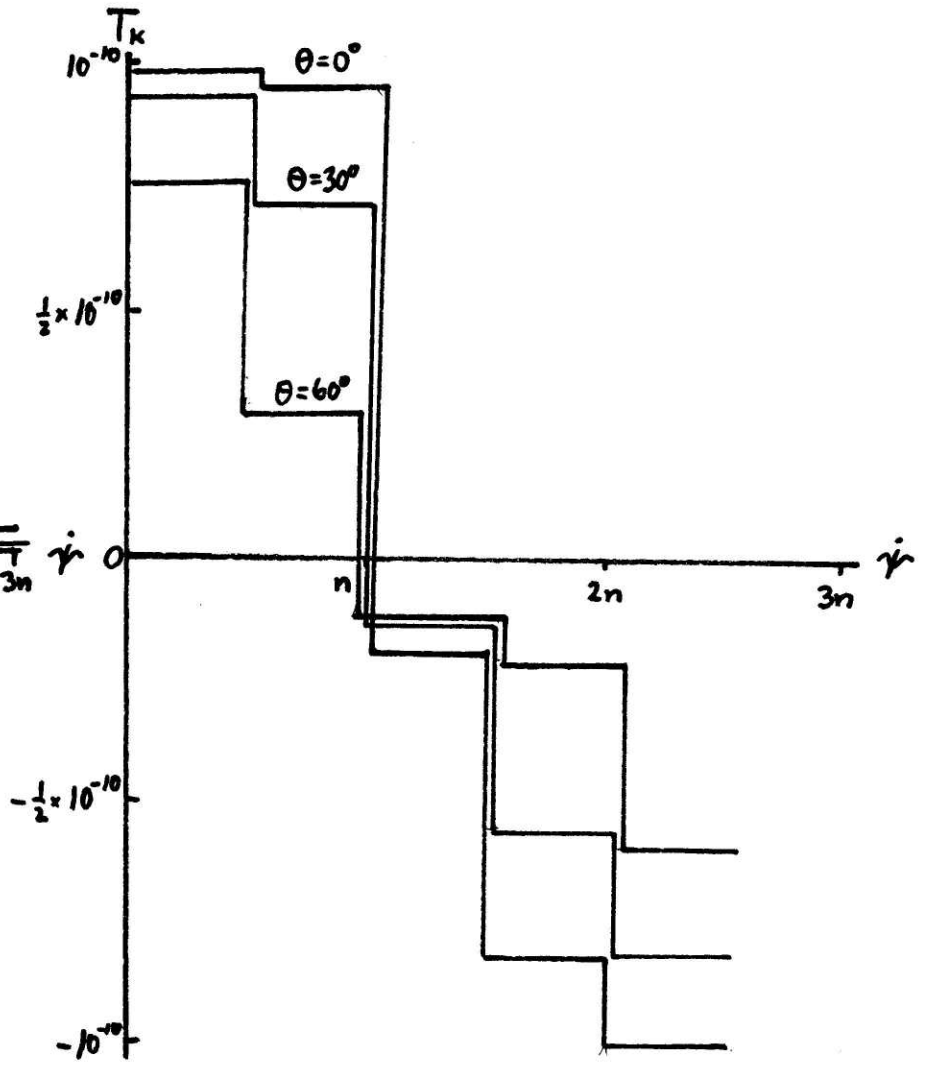


Fig. 9



a



b

Fig. 10

1  
∞  
1



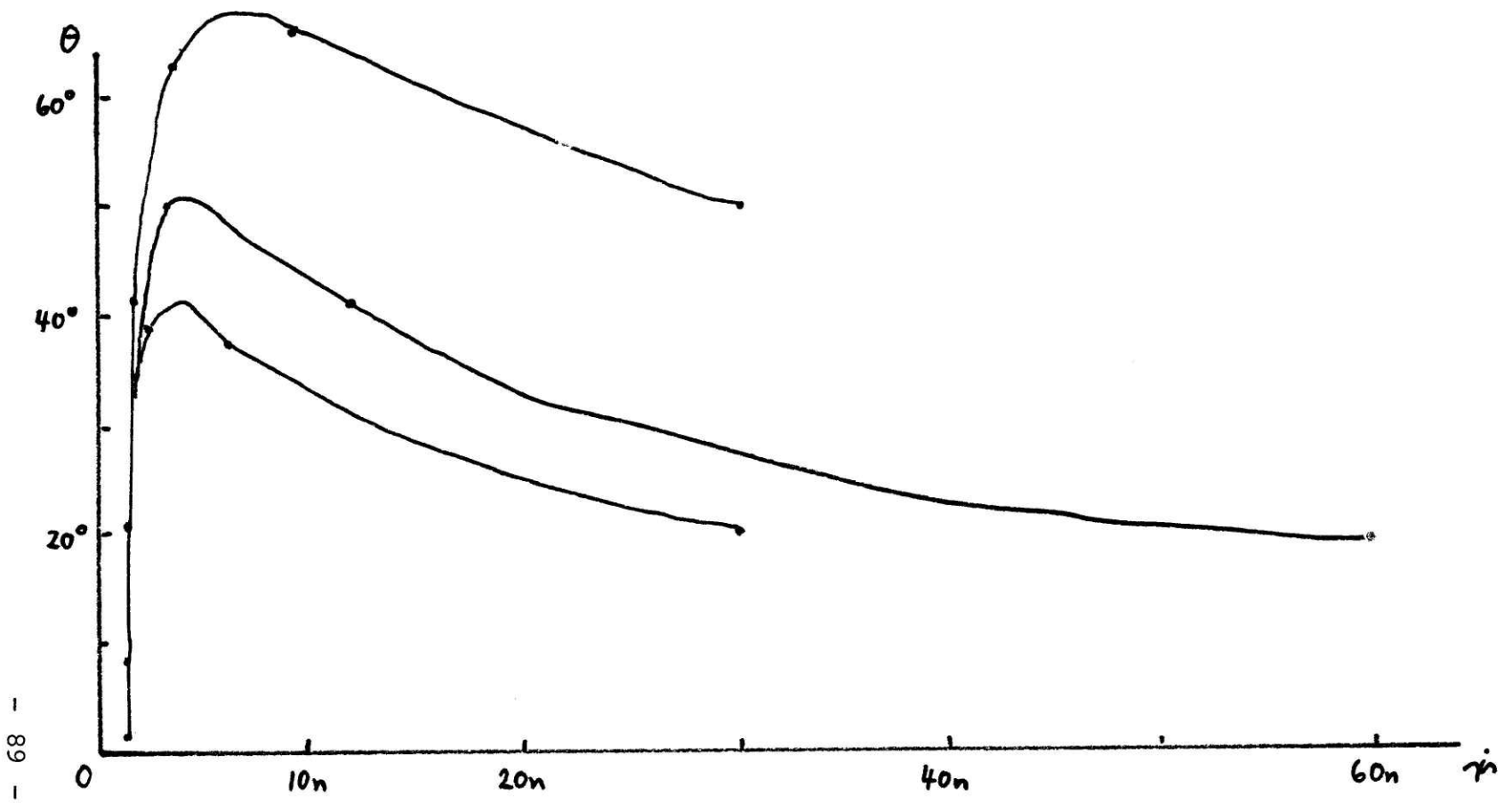


Fig. 11

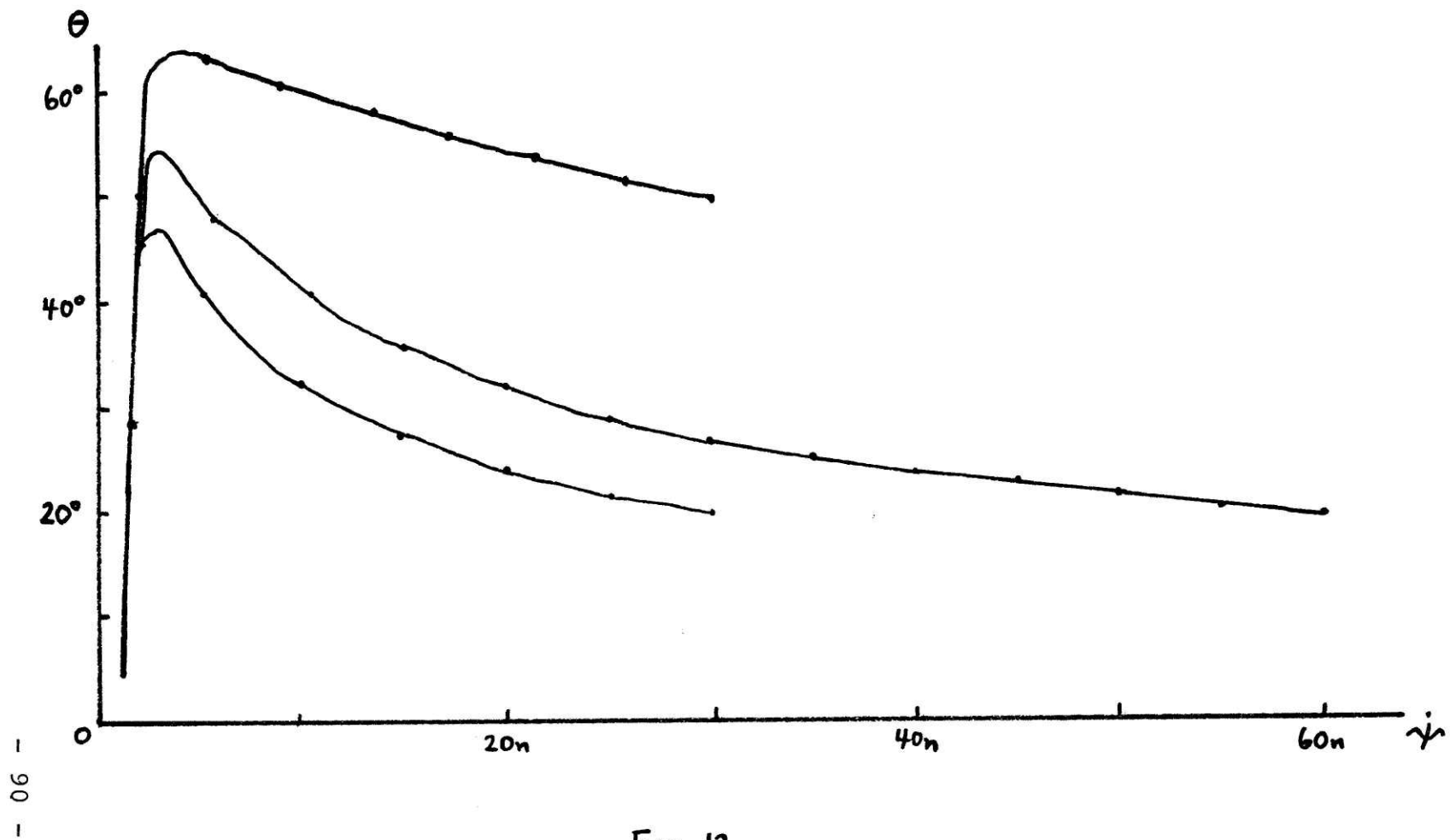


Fig. 12

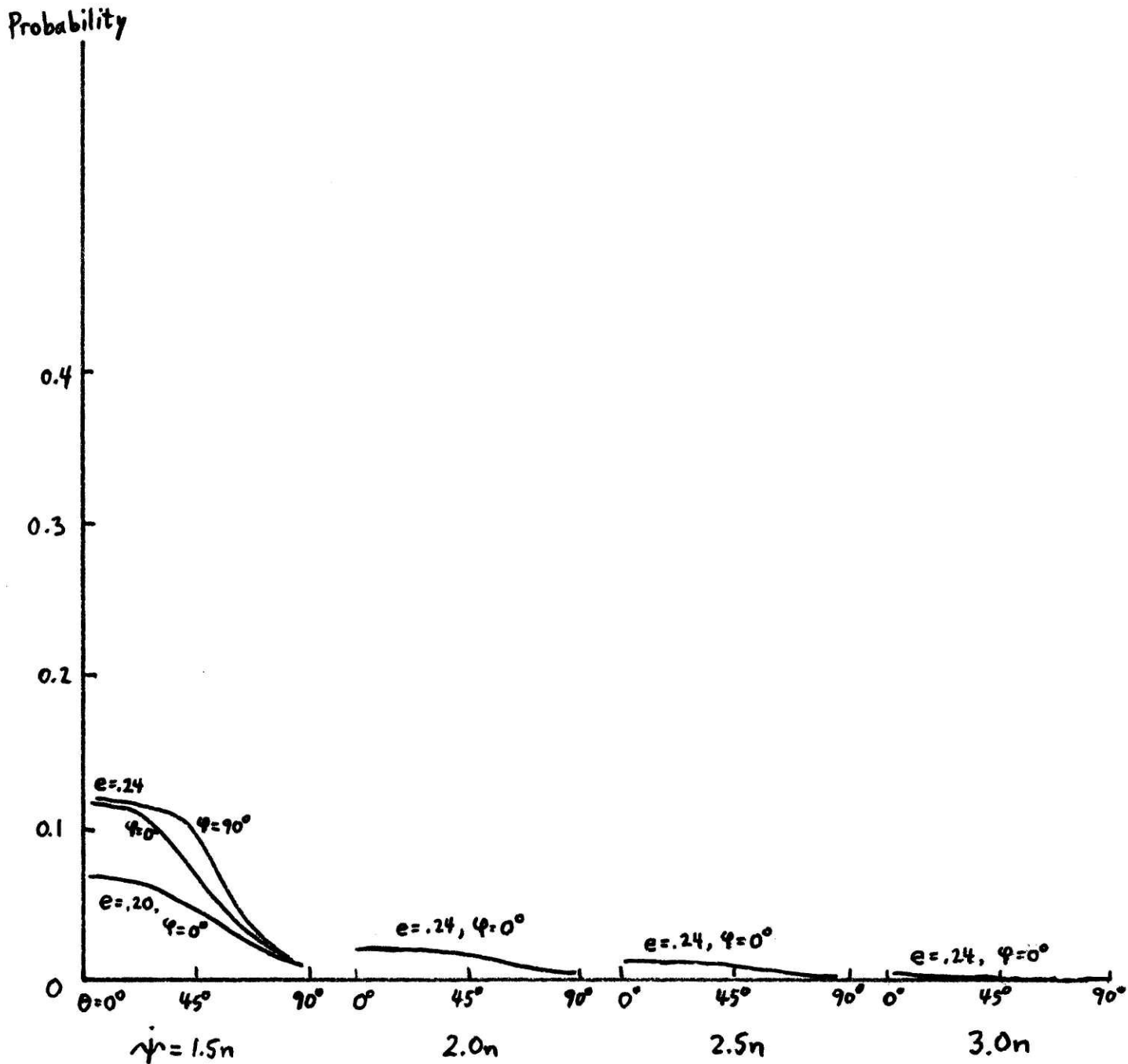


Fig. 13

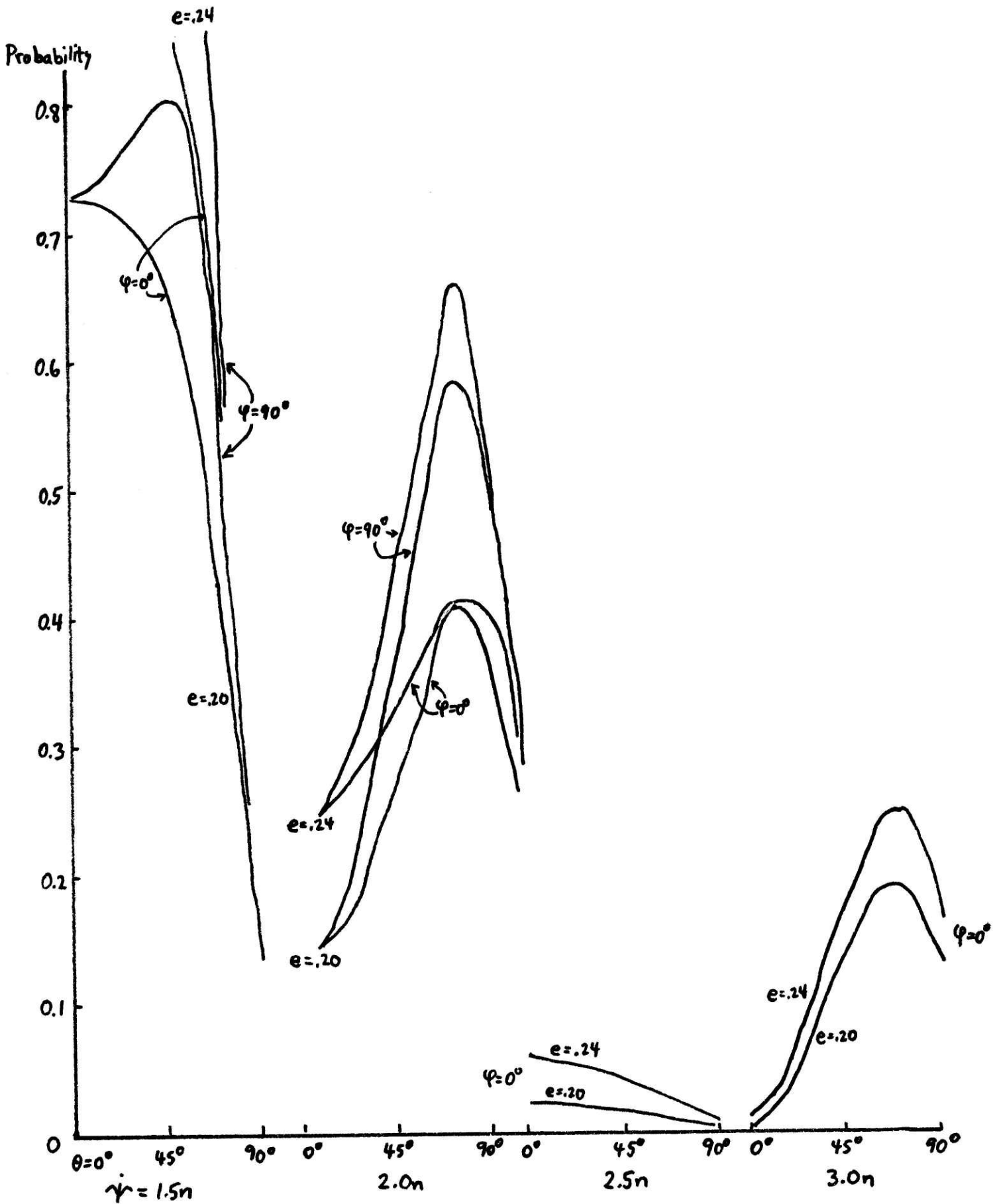


Fig. 14